THE UNIVERSITY OF QUEENSLAND

Bachelor of Engineering Thesis

Automated Digital Fabrication Concept for Composite Facades

Student Name: Judah HOOK

Course Code: MECH4500

Supervisor: Dr Michael Hietzmann

Submission date: 28 October 2016

A thesis submitted in partial fulfilment of the requirements of the
Bachelor of Engineering degree in Mechanical Engineeing

UQ Engineering

Faculty of Engineering, Architecture and Information Technology

1 Table of Contents

Abstract

The buildings we inhabit consume a considerable amount of the energy each year however there is currently a global movement towards minimising the impact human society has on the environment. This is driving the demand for more complex, and even intelligent façade systems to reduce the requirements of air conditioning and lighting while maintaining comfort. Through the development of 3D modelling and analysis software, architects and engineers have the ability to digitally produce innovative solutions. However, when complex, double curved geometries are proposed, the costs and difficulty associated with conventional fabrication techniques often make the transition to reality impractical.

Detailed within this paper, is the investigation and development of an alternative fabrication concept the utilises an inexpensive, reusable "pin board" mould that is autonomously set to various CAD derived surface geometries by a 6-axis robotic arm manipulator. A digital algorithm models a double curved test façade, subdivides it into manageable panels based on the dimensional parameters of the mould, creates a robotic toolpath simulation to map the surface geometry and generates the required machine-driving code.

Active trails successfully set the pins of the mould to within 0.6mm of the analytically predicted coordinate. At fully operational speeds, this process is estimated to take less than 2 minutes. To establish a proof of concept, automated setting of the mould was conducted for two neighbouring panels of the façade with unique but respective geometries. Under its design intent conditions, the set mould was used to fabricate samples of the digitally designed panels out of composite materials to assess the concepts strengths and weaknesses.

This resulted in geometries that adequately resembled the curvature of the CAD model, however preliminary samples exhibited considerable surface and structural defects. Alteration of composite material selection and minor mould modifications refined subsequent panels sufficiently to allow for their assembly. While imperfections still exist, the continuation of curvature from one panel to its neighbour exhibits good correlation and the assembled façade section can easily be identified from the digital surface.

At all stages of experimentally testing the concept, limitations were identified and addressed as far as practically possible. For those remaining, solutions are detailed such as design modifications and algorithm improvements, that if implemented in future works will aid the development of the automated fabrication concept, potentially towards a full-scale composite façade fabrication method that permits complex geometries while remaining cost effective.

Acknowledgements & Contributions

I would like to acknowledge my supervisor, Dr Michael Heitzmann for his intellectual input, guidance and support throughout 2016. While this project was not originally available as a thesis topic, when an alternative fell through Michael put forward this concept and agreed to take me on as an additional student. For this and the faith he placed in me, I will always be grateful.

To Ting Lee and Joe Gattas whom are credited for modelling the façade panel in Grasshopper and laying down a foundation for the project. I appreciate the time you spent and resources you provided, especially when conducting the preliminary trials with the robots and KUKA|PRC.

I would like to thank all members of the Architectural Workshop Group. John Stafford deserves mention for his insights into operation of the robots as well as conducting inductions, always being available to unlock the machines, assisting with the refinement of the mould and his general enthusiasm towards the project.

Special thanks go to John Milne whom is credited for the original design and manufacture of the pin board mould as well as the collaboration we conducted to come with improvements and solutions. He was instrumental in assisting with the fabrication of the sample façade panels in the final push to finish. Working with him was a great experience from which I gained valuable knowledge.

I would like to acknowledge Michael Dickson for the various robot related CAD models he provided.

Lastly I would like to thank my family and partner, Paige Hollenbeck for their unwavering love, support and encourage throughout the project.

List of Tables

List of Figures

Equation 2 – Modified Parametric Equation

List of Acronyms & Abbreviations

AD   Autodesk

CAD   Computer aided design

CAM   Computer aided manufacture

CNC   Computer numerical control

KRL   KUKA Robot Language

NURBS   Non-uniform rational Basis spline

PLC   Programmable Logic Controller

1. Introduction

Governed by The University of Queensland's, EAIT faculty is an endeavour, which involves the collaboration of multiple technical disciplines ranging from Architecture to Civil, Mechanical, Materials and Robotic engineering. The aim is to develop a system that is capable of fabricating façade cladding for a pavilion, which has a double-curved geometry as seen in Figure 1.
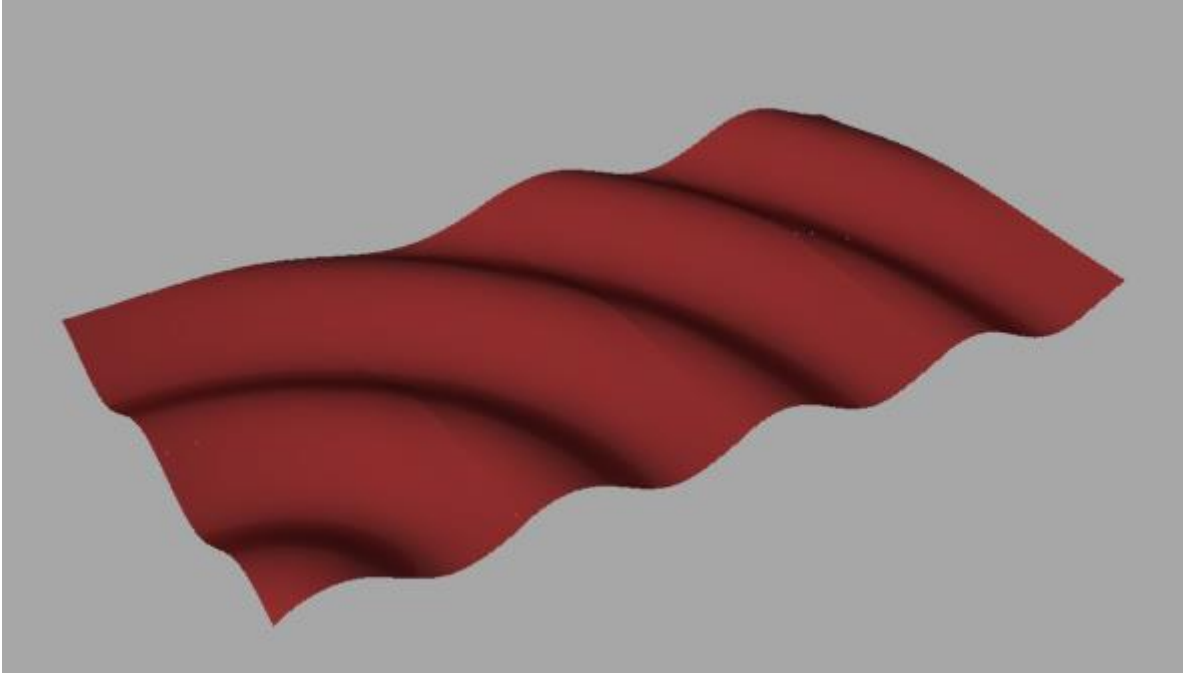
Figure 1 – Façade panel with double-curved geometry. (Source: Modified model of Rhino file supplied by Joe Gattas.)

While various, well established fabrication techniques could be employed to achieve this, the system in development aims to deliver an alternative approach to geometrically complex façade manufacture. The concept utilises a dynamic mould where manipulation allows the inner surface to assume variable, continuous contours. It is the design intent that these contours match a section or "panel" of the CAD modelled façade, the dimensions of which are defined by parameters of the mould. Furthermore, the manipulation or setting of the mould is driven autonomously through robotic actuation where the tool path is again derived from the CAD model. Hence, the robot will interact with the mould to replicate the digital surface of the segment that is followed by the introduction of composite material to form the corresponding panel. The process will iterate by applying sequential sections of the CAD model to produce the remaining panels each with unique geometry that are assembled to form the full structure. Figure 2 shows a visual illustration of the proposed process.
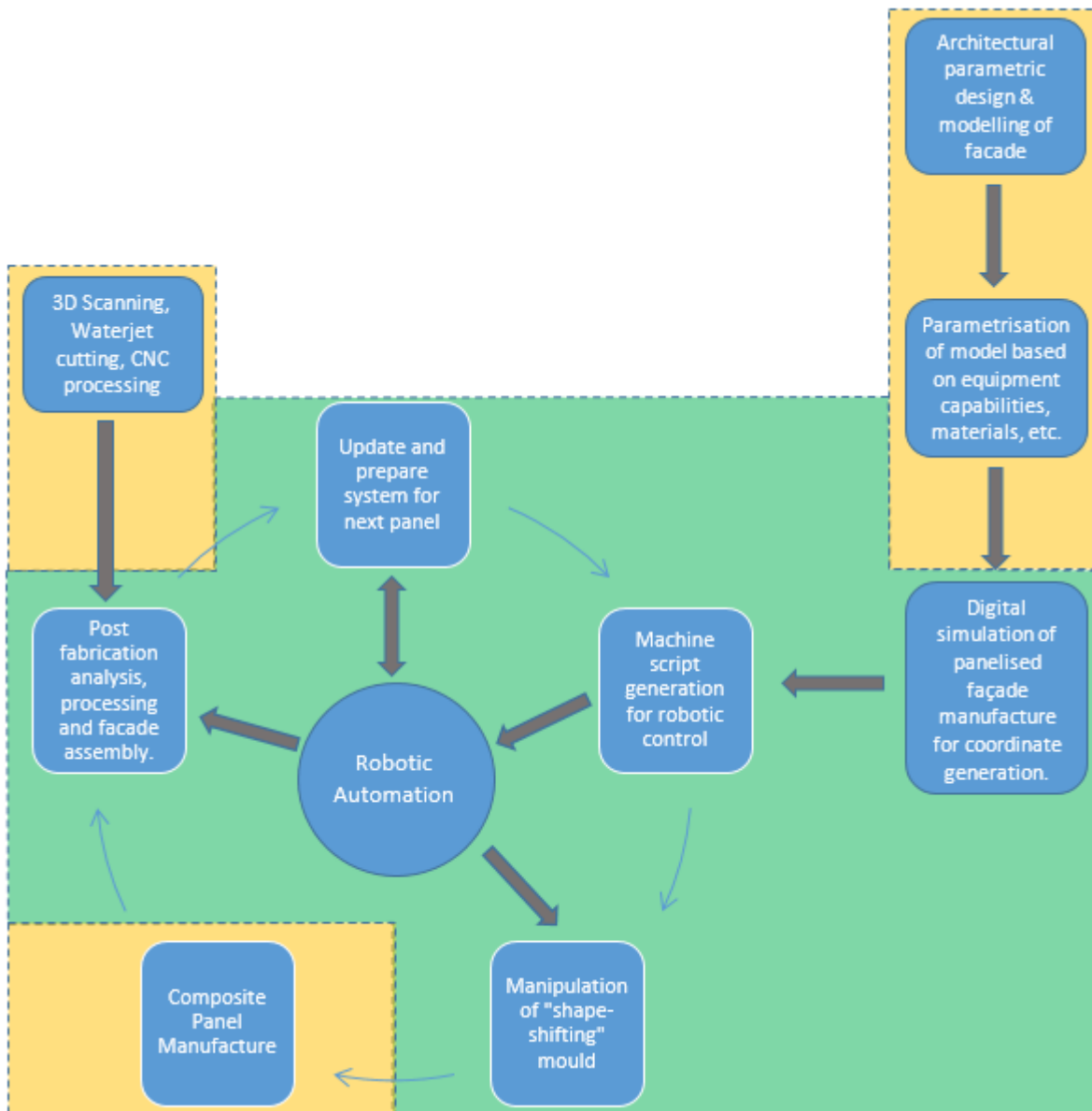
Figure 2 - Alternative approach to autonomous, digital fabrication of composite facades.

The EAIT faculty possesses two KUKA industrial robots, which up until this point have been underutilised. The highly versatile and flexible machines have been selected to meet the automation demands associated with the project. It is hoped that by completion, the endeavour will help justify the investment by providing the faculty with a competent team of operators and educational resources while sparking an interest to bolster the use of these research tools.

A successful outcome demonstrates a proof of concept in regards to the viability of using this approach for digital fabrication. It will establish a foundation for future avenues of research and concept development by the EAIT staff and students. This foundation has the potential to contribute to the emerging field of Robotics in Architecture as well as Architectural design and

manufacture for the construction industry. Reasons as to why this research may be significant are highlighted in the Literature Review.

2. Aim & Objectives

This thesis aims to investigate a concept for digital fabrication of composite façade panels by providing an autonomous solution that makes use of the robotic technology that the University of Queensland has invested in.

To successfully address the aim, the following objectives define the works required:

- Develop a software based solution that captures surface geometry from a CAD model and subsequently generates a stimulatory toolpath based on this information.
- Establish a means of transforming this toolpath into a format that can and used to drive the KUKA machines to physically replicate the surface in an adjustable mould.
- Use the mould to reproduce the surface geometry in the form of composite panels.

This is followed by an exploration into the potential of using the same robotic technology to conduct post fabrication activates such as refining the panels and assembling the façade. Finally, to determine if this is a viable approach for full-scale digital fabrication or more suitable for rapid prototyping.

3. Project Scope

3.1. Goals & Contribution

The compartments seen in Figure 2 were set out to define the scope of this project within the bounds of the greater endeavour. Aspects directly related to the primary aim of the thesis are bound in green and key goals associated with completing the underlying objective are to:

- Gain an appreciation for the significant role that façade design and manufacture has in the construction industry. This is focused towards complex geometries, how the two processes are currently achieved and what factors complicate the transition from concept to physical product.
- Determine the combination of software tools that are most suitable for robot operation in the context of the project based on the following criteria:
    - Accessibility, licencing and cost.
    - Level of technical support provided by the OEM and/or developers

- – Ease of use and associated learning curve.

- – Ease of system integration and functionality i.e. is an interface present for conducting robotic simulations that can be converted into machine code that drives the actuators correctly.

- – Resources i.e. has the software(s) been used, documented and published for similar applications.

- – Industry opinion

- Establish evidence to validate the autonomous digital fabrication concept by experimenting with the equipment and software available to produce two or more façade panels and subject them to an assessment against the CAD model. This allows for a sense of efficacy to be determined, in terms of achievable tolerances, product quality and limitations associated with the process.

- Produce a thesis document that effectively captures the key findings of the project so that contents can be used as an educational resource to guide students on how to effectively utilise the software and equipment. This will serve to reduce the learning curve required for further research conducted by others.

3.2.   Scope Boundary

Contents bound in orange indicate areas where an understanding is required but considered under the jurisdiction of other parties involved. Therefore, research, design, documentation and other technical aspects are addressed to a level of detail that benefits this thesis. The following list provides clarification as to what is consider out of scope:

- Any major changes to the current parametric design and modelling of the façade.

- Phase one design and manufacture of the mould is the responsibility of Mr. John Milne and Dr. Michael Heitzmann. As the robots will be interacting with the device to evaluate the concept, instructions related to its handling, assembly and operation need to be provided. Applying modifications to provide functionality, assessing the moulds capability and providing design improvements is considered part of the scope

- It is only necessary to know of and document the composite material used to manufacture the facade. Selection of the material and the processing required to use should be determined by persons with composite material experience.

- Post fabrication processes such as but not limited to 3D scanning, CNC machining and waterjet cutting shall be conducted by FWG technicians unless the student is approved to do so once the relevant risk assessments and inductions are completed.

4. Literature Review

A modern façade is loosely defined as the external envelope that encases the structural core of a building, separating the interior usable space from the external environment (Llinares-Millan, 2014). The components used can vary dramatically in complexity, arrangement and material when comparing one façade to another; however, each will attempt to serve similar functions. Examples of these include defining the architectural appearance of the building, providing the inhabitants with protection against the elements, transferring wind induced load into the structural core and many more (Knaack, 2007), a few of which are summarised in Figure 3.
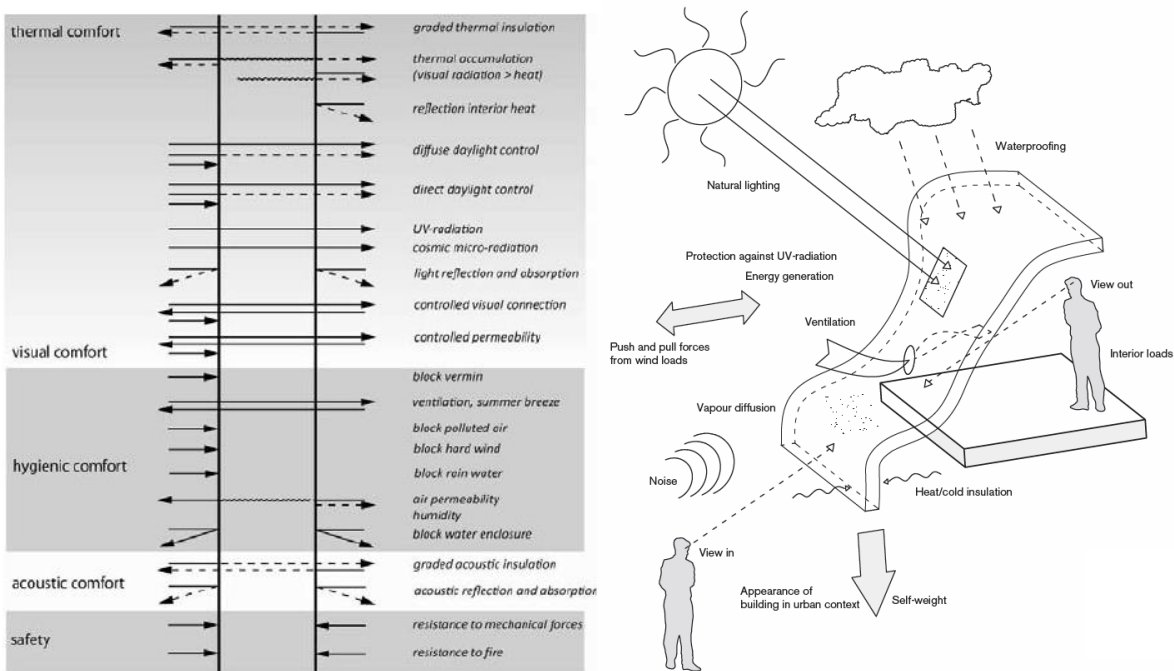
Figure 3 - Examples of facade functions (left) (Ginkel, 2010) and the influences they control(right) (Knaack, 2007).

The degree to which facades succeed at achieving these functions has increased over human history from the stone, stick and mud structures of the past to modern façade systems such as curtain walls. The environmental impacts that human activity is having on the planet are rapidly gaining more attention and shaping the future of many industries including construction. This is driving the demand for more "intelligent" facades that not only cope with but also respond to environmental changes. Take for instance the Al Bahar Tower's in Abu Dubai that has an

actuated façade system comprised of many triangular panels that fold in response to optimum light and solar conditions throughout the year. It has been estimated that provide up to a 50% reduction in the energy required by air conditioning systems used to maintain internal thermal comfort.

Figure 4 - Actuated, folding facade of AL Bahar Towers (Source - http://www.archdaily.com/270592/al-bahar-towers-responsive-facade-aedas)

Advancements in computer aided design and software development has empowered architects and engineers with the ability to develop state of the art solutions such as this. It allows them to envision complex geometries that are free form in nature for use in their work. The problem is that the designs are stretching the capabilities of the fabrication industry as while conceptualising the shape is easier, physically creating the objects can be challenging and expensive.
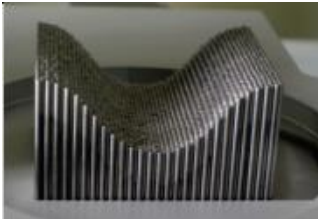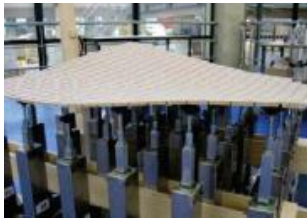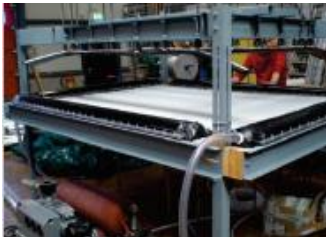
Take, for example the Nordpark stations in Austria where the 850 glass façade panels are of a unique, often double-curved geometry. A static mould was created for each using steel rods contoured to the desired shape and an 8mm thick panel of glass thermoformed to create a smooth surface covering the rods. Finally, 12mm thick panes were heated until malleable and set in one of the 850 moulds followed by white layer of polyurethane resin. While this does not describe all aspects of the construction of the four stations, it is easy to appreciate why the project cost has been estimated at £36 million (Spring, 2007). A study into cost estimation and panel optimisation of free-form building facades used in South Korea concluded that double-curve geometries cost twice that of single curvatures due to the complicated fabrication processes required (Park, 2015). Developers often impose restrictions on architects because of this and only specialised projects with extensive budgets can produce artistic, innovative structures like those of the previous examples. This will remain the case until an economically

viable moulding technique is developed that is reusable and provides the flexibility to produce complex geometries.

Additive techniques, such as 3D printing and subtractive methods, such as CNC milling and grinding are part of the façade fabrication arsenal (UQ - School of Civil Engineering, 2016) (Llinares-Millan, 2014). However, research for this project is focused on formative approaches and further specified to mould based manufacture as it forms a building block of the concept.

The idea of a "shape shifting" mould is not novel and dates to its first inception by Leonardo da Vinci. The concept for adjustable mould have been investigated by several others such as the FlexiMould by Beors (Boers, 2016), the model designed by Reitbergen and Vollers (Pronk, 2009) and that created by Pronk. In general, the moulds consist of a stretched membrane or spring steel mesh, which is shaped using uniformly distributed, height adjustable pins or inflatable tubes or simply using the pins themselves to form the desire surface. **Table 1** illustrates examples of the different flexible mould concepts that have been investigated in the past.

Table 1- Examples of currently investigated flexible mould concepts

Flexible mould method	Examples
Pin-bed surface	*Figure 5 - FlexiMould (adapted from Boers)*
Supported flexible layer	*Figure 6 – Adaptable mould (adapted from Reitbergen & Vollers)* *Figure 7 - Spring Steel Mesh Mould (adapted from Pronk*
Tensioned flexible layer	*Figure 8 – The "E-Mould" in undeformed position (adapted from Van Rooy & Schinkel).*

The dedication by these researchers conveys how this is a problem for which an effective solution is eagerly sought. Their efforts have all been successful in their own right however, one issue consistently encountered is finding a balance between the accuracy of the surface which is dependent on the number of actuators and the cost associated with using a large number as shown in **Error! Reference source not found.**.
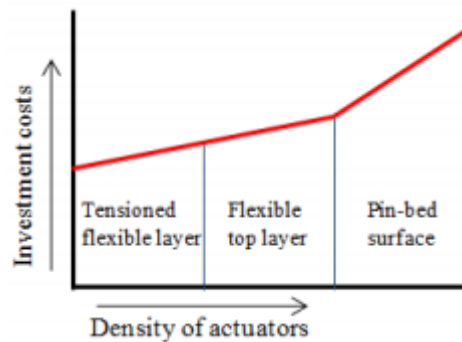
Figure 9 - Relation between density of actuators and investment costs (Pronk, 2015)

Currently research indicated that a situation whereby robotic arm automation has not been used to replace the actuators of these moulds. Thus the proposed concept appears to be a novel approach at overcoming the issue of controlling the mould. A solution would be beneficial as the moulds could be simplified to reduce costs while increasing the functionality of the system as the robots could be used to not only manipulated the mould but also for façade assembly and post fabrication refinement.

5. Equipment Summary

The purpose of this section is to outline the KUKA robots, their specification and to outline why their capability suit the autonomous functionality required by the proposed concept. It also serves to summarise the details of the pin board mould that is being developed by John Milne for the Composites Division at UQ.

5.1.   KUKA Robotic Manipulators

The two KUKA Industrial Robot models that are available for use are the KR 16-2 and the large, high precision KR 30 16-2. The first is considered as a low payload machine and the later as a medium payload machine however both are rated to carry payloads of 16 kilograms which is more than sufficient for manipulating the pin board and relocating façade panels. Figure 10 summarises the keys specification details for each model obtained from the relative KUKA specification documents.

	KR 16-2
Max. reach	1,611 mm
Rated payload	16 kg
Rated suppl. load, arm/link arm/rot. column	10/variabel/20 kg
Maximum total load	46 kg
Pose repeatability	±0.05 mm
Number of axes	6
Mounting position	Floor, ceiling, wall
Variant	🟠, 🟦
Robot footprint	500 mm x 500 mm
Weight (excluding controller), approx.	235 kg

Axis data/ Range of motion		Speed with rated payload 16 kg
Axis 1 (A1)	+/-185°	156°/s
Axis 2 (A2)	+35°/-155°	156°/s
Axis 3 (A3)	+154°/-130°	156°/s
Axis 4 (A4)	+/-350°	330°/s
Axis 5 (A5)	+/-130°	330°/s
Axis 6 (A6)	+/-350°	615°/s

	KR 30 L16-2
Max. reach	3,102 mm
Rated payload	16 kg
Rated suppl. load, arm/link arm/rot. column	35 kg/-/-
Rated total load	51 kg
Pose repeatability	±0.07 mm
Number of axes	6
Mounting position	Floor, ceiling
Variant	🟠
Robot footprint	850 mm x 950 mm
Weight (excluding controller), approx.	700 kg

Axis data/ Range of motion		Speed with rated payload 16 kg
Axis 1 (A1)	+/-185°	100°/s
Axis 2 (A2)	+35°/-135°	80°/s
Axis 3 (A3)	+158°/-120°	80°/s
Axis 4 (A4)	+/-350°	230°/s
Axis 5 (A5)	+/-130°	165°/s
Axis 6 (A6)	+/-350°	249°/s

Figure 10 - KUKA robot model specifications (adapted from the KUKA Specification Documents)

Considering the details above in conjunction with the work envelope diagrams in Appendix 8 for each model, the dimensions of the mould are well within their respective ranges of motion. The KR 16-2 model may prove more suitable for single panel fabrication due to higher rotational speeds and the better pose repeatability. This will improve the working times required to manipulate the mould and the accuracy achieved between iterations. Based on this rationale and as the project focuses on establishing a proof of concept where live automation is limited to setting the mould, any mention of a robot in subsequent sections is referring to the KR-16 model unless otherwise stated. The KR 30 16-2 has more than double the reach of the KR 16-2 and so will be more suitable for façade assembly and post fabrication machining. How best to approach this integration will be investigated while gaining experience with the machines and through researching their KR C4 control systems (KUKA Robotics Pvt Ltd, 2016).

Through exploring the book "Robotic Fabrication in Architecture, Art and Design 2014" by Wes McGee et al, it has become clear that these machines can provide the functionality required to complete the project. The challenge is bridging the knowledge gap required to effectively operate the machines. A, paper titled "Variable Carving Volume Casting – A Method for Mass-Customized Mould Making" contributed by Brandon Clifford and associates provided the most confidence in the machines. For this project, the team programmed a KUKA machine with similar specifications, to carve a complex negative geometry from EPS foam (McGee, 2014). The result of the endeavour is shown in Figure 11.

Figure 11 - Example of the KUKA Robot capabilities []

5.2. Pin Board Mould

The pin board mould for this project, developed by Mr. John Milne and Dr. Michael Heitzmann, is similar in design to those previously discussed. It relies upon a network of pins capable of linear movement along the z-axis. A ball bearing is secured to a terminal end of each pin which acts as the joint between the pin and it respective hexagonal plate. Magnets secured to the underside of the plates establishes a connection with the bearing to provide three degrees of rotational freedom. In total 162 pins are inserted into a wooden box frame through an offset grid of holes with inter-pin dimensions shown in the bottom image of Figure 12. The offset is deliberately included to provide 25mm of overlap between panels to ensure and accurate match between the married edges of neighbouring panels once cut to size. This forms the adjustable component of the mould with which the robot interacts to displace the pins by a CAD derived distance to produce the desired contour.

To ensure that the plates which form the contour, do not leave deformations in the fabricated panels, a 5mm silicon membrane is clamped between the support frame and mould top. This

support frame is partially inserted over the pin board box once the pins are set. This forms a cavity that encases the contour so that when a vacuum is introduced to the pin board box, the resulting negative pressure stretches the silicon over the hexagonal plates. The upper surface of the tensioned sheet forms the mould tool upon which composite facades panels are shaped. provides visual identification of the individual components and their assembly to form the completed mould. To avoid repetition of images, those that portray results significant to the project are presented further in this document. Note that as three hexagonal plates had not been fabricated, a single row of pins was removed from the boundary which has no significant impact on the findings detailed in this report.
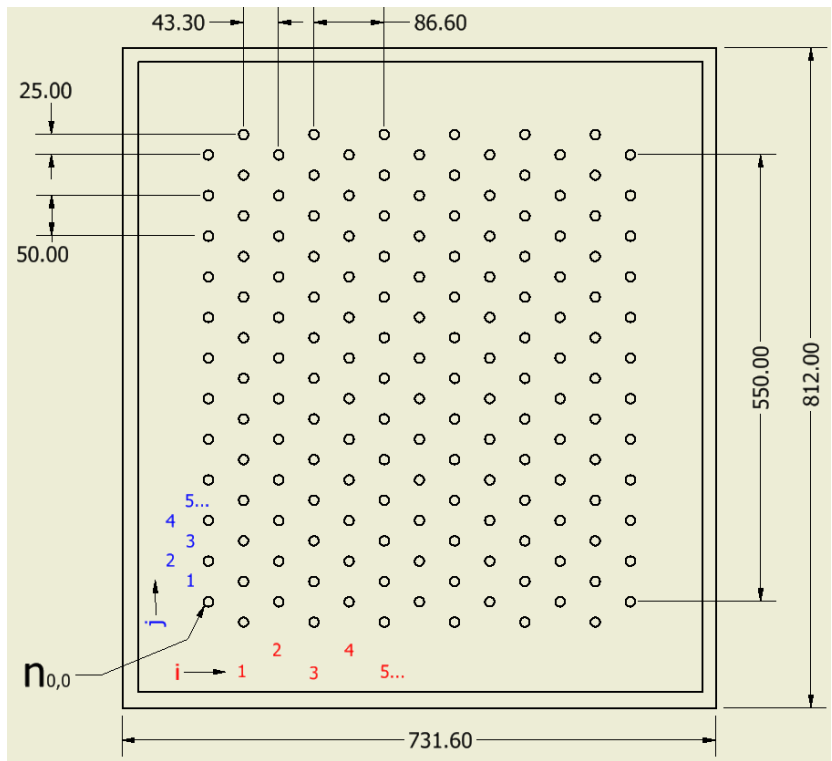
Figure 12 – Mould components and assembly: Ball bearing topped pins in board frame at zeroed position (top left). Support frame with secured silicon sheet inserted over pin board mould (top right). Board / offset grid dimensions with pin coordinate system (bottom).

6. Software Review

6.1. Selection Criteria

6.2. Assessment of Secondary Software Options

1.1.1 RoboDX

Unfortunately, this section could not be written up prior to the due date.

1.1.2 Autodesk Revit & Dynamo

Revit is a member of the family of products developed by Autodesk, Inc. Its primary purpose is as a building information modelling software used extensively in the construction industry. Dynamo is analogous to Grasshopper in that it is a visual programming editor and for the purposes of this project provides the same functionality albeit with different functional block definitions. Due to this similarity and the fact that Autodesk provides an extensive suite of programmes free of charge to student, it remains a potential software option to keep in mind for future use.

The Primer for Dynamo v9.0 and the introductory video tutorials (AutoDesk, Inc, 2016) are the two major resources relied upon. A key difference between the two editors is that dynamo can operate as a Revit plug-in or an independent application where the geometry and block code is stored in different layers on the same screen shown in Figure 13
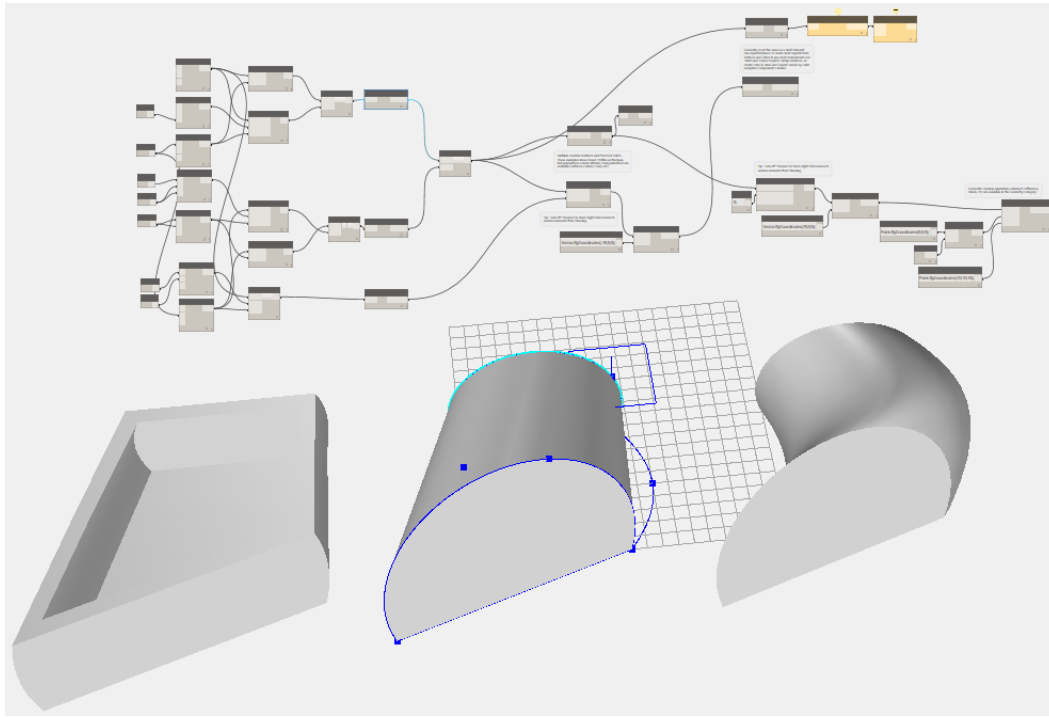
Figure 13 - Curved Surfaces Tutorial, Code & Geometry

The significance of this is that often errors occurred when attempting to observe the output of Dynamo algorithms in Revit. Figure 14 illustrates an example of this where only the right hand shape is modelled. This proved frustrating to overcome and could be due to either inexperience or the fact that Revit is not a NURBS based modeller. Furthermore, as BIM software it has the functionality to incorporate building services into the architectural design. While useful to the construction industry, these aspects are not relevant to this project, and make Revit difficult to navigate, and so it appears less suited compared to its competition, Rhino.
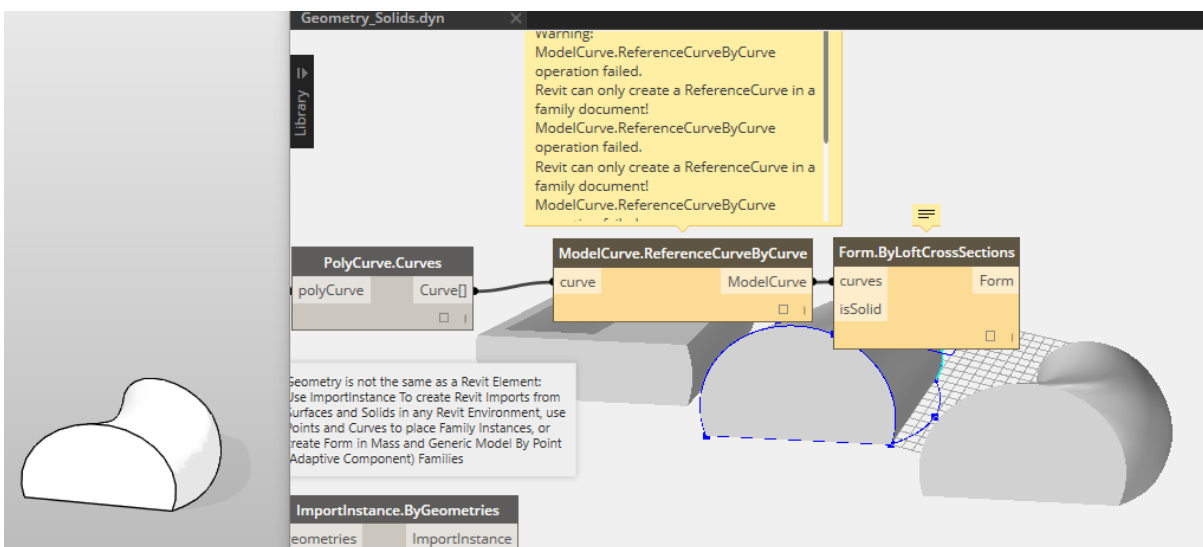
Figure 14 - Revit modelling issues

The primary reason that additional work with dynamo was put on hold after completing the introductory tutorials is that a communication interface between the software and robots is not presently available. Misleading advice was obtained from a junior technical support office for KUKA Robotics Australia who stated that a technology called MxAutomation could provide a solution. Further investigation uncovered that this software is to interface KUKA equipment with external programable logic controllers (PLC) produced by companies such as ABB and Siemens and is has so relevance to Dynamo or the project. During the 2016, Association for Robotics in Architecture (ARA) Conference, refence was made to software extension that will allow dynamo to conduct robotic simulations however there are currently no reliable resources that detail the plug in or discuss a potential release date. Thus, in the context of this project, Dynamo was removed as a possible option.

7. Selected Software & Algorithm Generation

7.1.   *Rhinoceros 3D & Grasshopper*

Rhinoceros 3D or Rhino, developed by Robert McNeel & Associates, is a CAD application that generates digital geometries based on the NURBS mathematical model. It is recognised as a market leading free-form modelling software that is utilised by a wide variety of industries including architecture and engineering. Grasshopper is a visual programming, node based editor that operates as a plug-in to Rhino. It provides the user with the ability to map out generative algorithms without the need for extensive mathematical or script based coding knowledge. The desired outputs are automatically reflected in Rhino by modelling the geometry derived from the algorithm. Incorporating various algorithms can allow for complex functions and even sub-programs to be developed, a good example of which is KUKA|PLC.

David Rutten, an employee of Robert McNeel & Associates and the creator of Grasshopper, provides a thirteen-part video tutorial series that helps the user grasp a foundational understanding of the plug-in (Davidson, 2016). These along with The Grasshopper Primer (Issa, 2009) have been referred to extensive as part of skills development.

The remainder of this section serves to highlight how the lessons learned from the Grasshopper resources, aided in becoming familiar with the work conducted by Joe Gattas and Ting Lee whom are credited for modelling the ripple façade panel previously seen in Figure 1. Additionally, KUKA|PRC is introduced as the primary robot simulation tool for the project and is discussed in detail. Appendices 1 to 4 are annotated extracts from Grasshopper that serve as

a functional description of the code and should be referred to with continued reading. The first provides a holistic view of the initial form used for preliminary simulations in the early phases of the project. Appendices 2 and 3 provide detail on components that are specifically responsible for modelling the façade surface. Appendix 4 is the section of the algorithm that makes use of KUKA|PRC functional blocks for conducting the preliminary simulation.

7.2. Façade Modelling & Panalization Algorithm

The defining parametric equation for the geometry of the ripple façade is included below as Equation 1 alongside a 3D plot.

$$70 \times 0.6 \sin\left\{ \sqrt{\left(\frac{x+3}{8.0 \times 10^{-3}}\right)^2 + \left(\frac{y-1.5}{8.0 \times 10^{-3}}\right)^2} \right\}$$
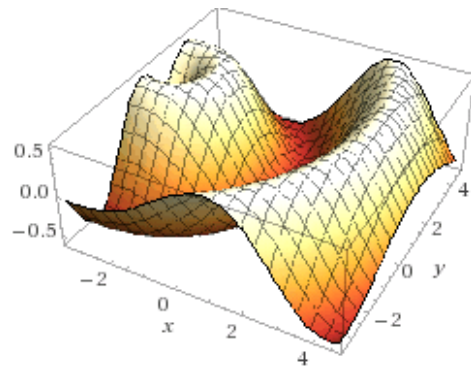
Equation 1 - Parametric Equation for ripple façade   *Figure 15 - 3D plot (Source: Wolfram Alpha)*

Ting Lee provided access to multiple Grasshopper files that over several iterations, had progressively lead to the generation of the ripple façade algorithm. See Appendices 1 to 3. It's description in short, is that a starting point is set for the first panel at Cartesian coordinates (x=0, y=0, z=0). Panalization is achieved by incrementing along the x and y axes by the respective inter-pin spacing (43.3mm, 50mm) and constraining by the number of pin rows and columns seen previously in Figure 12. This forms a distributed grid of points derived from the dimensional parameters of the pin board. These x and y values are then used as inputs in the parametric equation to obtain the corresponding z value of the ripple surface. By applying the "Curve Interpolation" and "Lofting" functional blocks in Grasshopper, the surface geometry of the first panel is constructed from these coordinate sets. The three resulting corners (x_max, 0, z), (x_max, x_max, z) and (0, x_max, z) are then used as the starting points for subsequent panels as shown. The synchronous repetition of the base algorithm models the eight panels that make up the façade cladding where Figure 16 shows that each panel, through its central plane, is defined by the dimensional parameters of the mould.
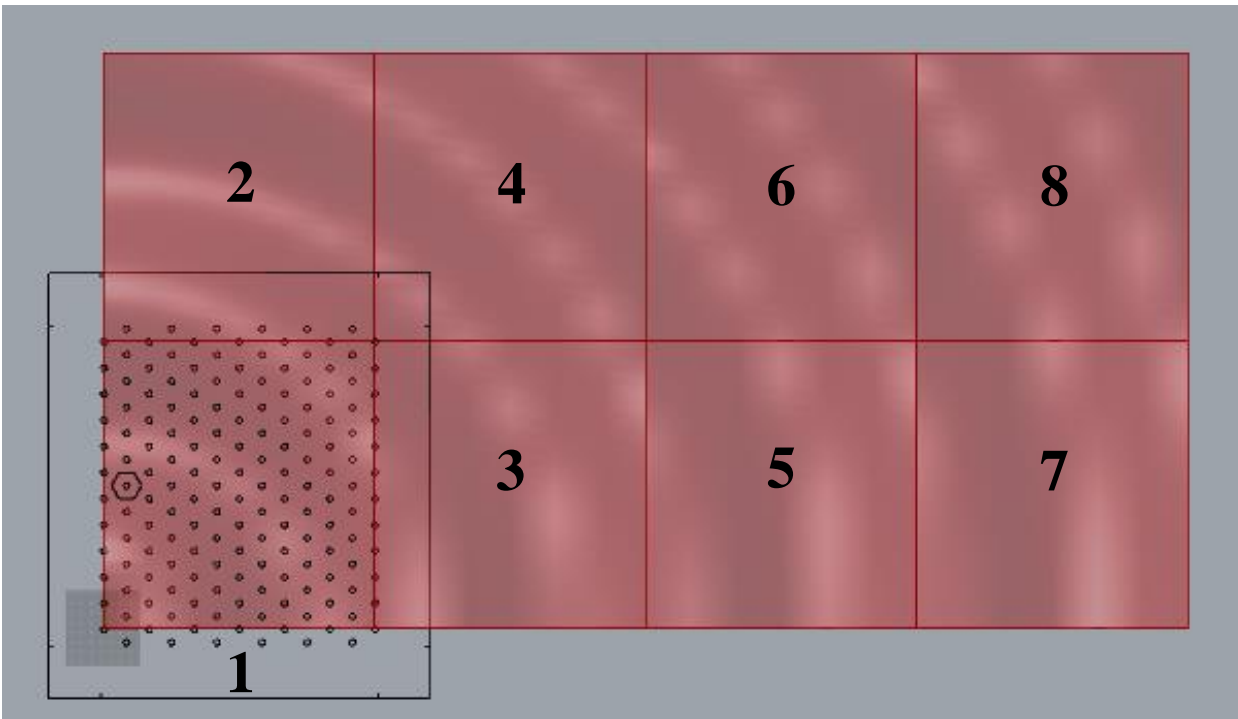
Figure 16 - Panelised ripple facade with overlayed pin board schematic (Source: Modification to files supplied during handover with Ting).

With the surface constructed, the (x,y,z) coordinates matching the pin locations are extracted and ready for use in robotic simulations.

7.3.   KUKA|PRC & Preliminary Simulation Algorithm

KUKA Parametric Robot Control is a Grasshopper based tool allowing the direct integration of the robots, which provides a communication interface that permits a transition from design to simulation and finally real-time automation. The application allows for input of the robot model and tool, which are automatically rendered in Rhino 3D. To conduct accurate simulations, various parameters are set in KUKA|PRC. This includes but is not limited to defining the "base" relationship between robot and facade, operational speeds and tool orientation of approach.
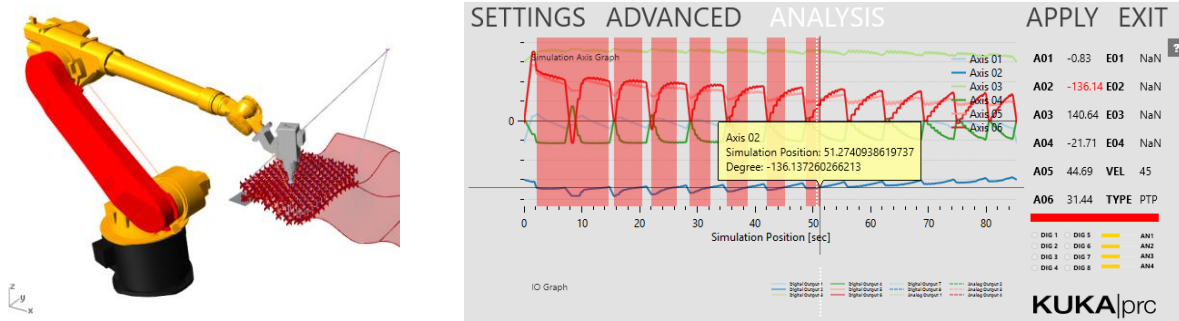
Figure 17 - Simulation analysis indicating kinematic errors

An extremely useful aspect of the program is the ability to analyse the simulation for motions that are outside the work envelope of the machine or those that result in component collisions. Furthermore, the analysis tool maps all the rotations required by each actuator to follow the toolpath and identifies singularities without the need to solve the complex kinematic equations that define the robot's ability. Overcoming obstacles such as these is essential, as the software will not generate the required KRL machine code until the issues are resolved. Figure 17 illustrates an example where multiple pin coordinates attempted to impose a rotation outside the bounds of axis two's range of motion. By redefining the base coordinates so that the robot is located further in the negative x-axis with respect to the facade, this kinematic breach is resolved as seen in Figure 18.
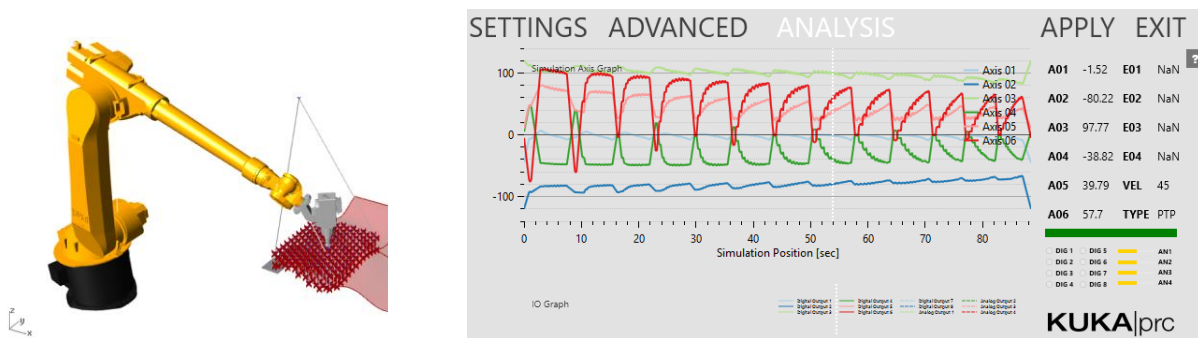
Figure 18 - Resolved simulation

Using the functional blocks included with KUKA|PRC, the façade modelling algorithm was extended to produce a simulation of the mould manipulation toolpath for the first panel, which was used in a preliminary active trial held on the 8th of April. With reference to Appendix 4, a point is set at the origin (0,0,0) of the panel to provide a reference for the simulation. The robot input coordinate set is deconstructed and the z values in the data stream overwritten with a user defined "Safe Distance" to establish a series of planes above the surface geometry that align with the x and y coordinates of the pins. This is the initial step in the robot toolpath generation. Consider the pin ($n^{0,0}$) located at the defined origin of the surface and thus the board where the modified z coordinate establishes a height above this pin that is common to the rest. This is where the negative linear displacement in the z-axis begins in order to push the pin into place. The distance at which the displacement terminates is defined by establishing a second plane for this pin based on the original input coordinate set (i.e. on the surface of the geometry). Next, a point to point motion is used for the transition from the surface plane of the pin ($n^{0,0}$) to the safety plane of the next pin ($n^{0,2}$) in the positive y-axis. The combination of these two motions iterates sequentially for each pin ($n^{0, j+2}$) in that column. Once the final pin ($n^{0, 22}$) is reached

[$(n^{i(odd), -1:23})$ for odd columns], a linear motion in the XY plane aligns the robot tool with the "boundary" pin ($n^{1,-1}$) of the next column. The algorithm progresses in this manner until all 162 pins have been set in the simulation. A portion of the toolpath generated by this process is shown in Figure 19 to provide clarity.
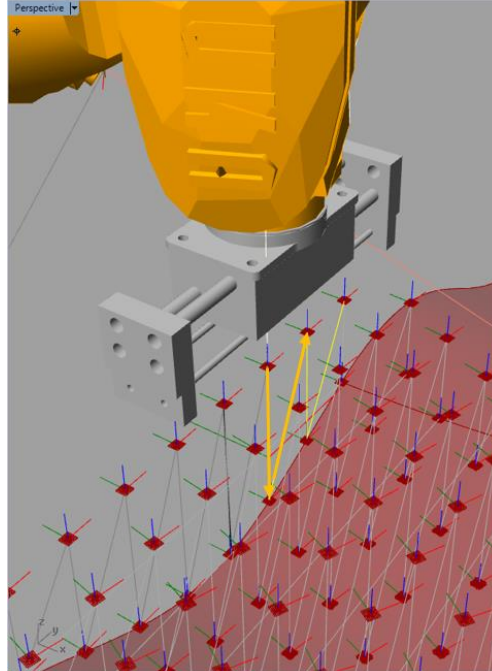
Figure 19 – Sample toolpath from preliminary simulation.

By setting the Output Directory (See Appendix 4), KUKA|PRC automatically generates the KRL machine-driving code and the script obtained for this simulation, once uploaded to the CR-C4 control system, did to engage the KR-16 actuators. The trial was marginally successful but it provided useful insight into aspects of the simulation and machine operation that were targeted for improvement.

Firstly as seen in Figure 19, the compressed air gripper attached to the robot is not suitable for displacing the pins, as the dimensions of the body are greater than the inter-pin spacing of the mould. Unless modified this would result in undesirable interactions with multiple pins in a single motion. Furthermore, by assessing the toolpath in Rhino, it also became clear that the point-to-point motion between pins would result in a collision between the tool and subsequent pin. Thus it was determined that both the tool and sequence of motions required modification.

However, the most concerning issue was that the motion of the robot in reality did not reflect that of the simulated toolpath and resulted in the breach of soft limits causing the robot to seize. Established during commissioning of the machine, these limits restrict the range of motion to avoid collisions with the table and boundary cage, the latter of which ensures the safety of the

operator. As the cage and limits provide essential layers of protection, an important consideration was that any improvements made are applicable within the confinement of these safety mechanisms. An additional problem encountered aside from inconsistent target coordinates, was that the orientation of approach by the robot tool was also erroneous. Hence, there was fundamental mismatch between the simulation and reality even though no error were detected by the Analysis function. The solutions applied to overcome these issues, are discussed in the following section.

8. Overcoming Preliminary Obstacles

8.1.   Gripper Extension Modelling and Fabrication.

For precise manipulation of an individual pin without disturbing those that surround it, an extension that attaches to the compressed air gripper is required. Michael Dickson produced a series of three wood extensions in duplicate for a different project involving the robots. These are unitised in conjunction with 25mm protrusions obtained by halving PVC pipe with a 18mm internal diameter which are fixed to 30 by 65 by 70 mm blocks of pine with tapped holes which are used to secure the components to the gripper. The high degree of flexibility associated with the PVC proved problematic so halved 15 mm chrome plated steel has been fixed to the internal surface of the PVC to add rigidity. This is followed a layer of non-slip mat secured to the metal in order to provide grip. When the compressed air gripper is engaged, the two halves of the piping assembly comes together to clamp on a 25mm length of 15 mm diameter pine dowel as shown in Figure 20. Manual experimental confirmed that the frictional force generated between the dowel and non-slip surface is sufficient to overcome that associated with the pin and mould frame interface.

With the tool extension in place, further active experimenting with the robots revealed an additional problem. During operation, the control system constantly monitors the precise state of the actuators via highly sensitive feedback loops. This includes variables such as rotational speed, torque, force generation and so on. Attaching the "unknown" extension to the robot, introduces additional inertial components that alter the expected system dynamics. When running a simulation, the robot responds to these discrepancies by halt its motion and reporting the following error message on the SmartPAD: "Tool Overload Detected".
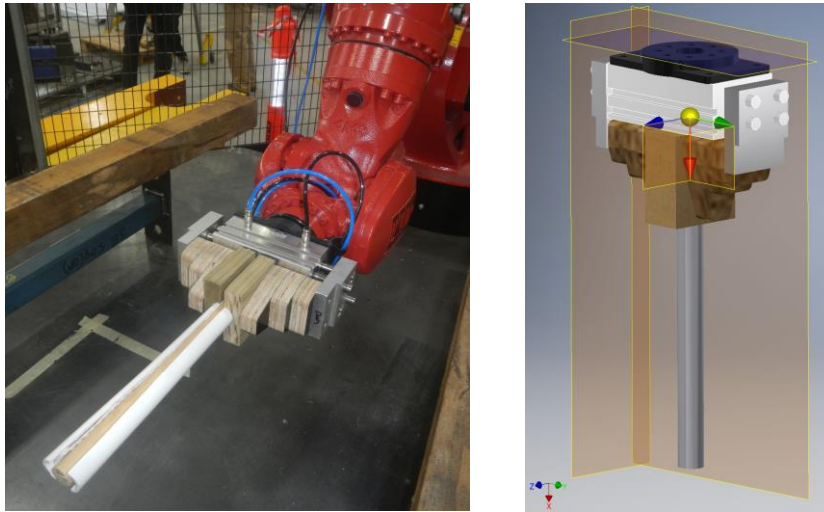
Figure 20 – Gripper extension prototype attached to robot (left) and Autodesk Inventor model (right)

When exploring the requirement for tool calibration detailed in the next sub-section, the option to define physical attributes of the tool provided a solution to this problem. The variables required include the mass, centre of mass and moments of inertia about principal axes. To obtain these values, a CAD model of the tool was generate in AutoDesk Inventor 2017 and appropriate generic material properties assigned to each component from the built-in materials database. As no information was available regarding the internal mechanism of the gripper body it is modelled as a solid block and fixings were neglected to offset the additional mass. The 3D model is shown in Figure 20 with estimates for the required variables in Table 2.

Table 2: Physical Attributes of Gripper Extension Inventor Model

General Properties:	Material:	Combination
	Ave. Density:	1.897 g/cm^3
	Mass:	1.777 kg
	Area:	0.237 m^2
	Volume:	0.001 m^3
Centre of Gravity:	X:	0.054 m
	Y:	0.094 m
	Z:	0.032 m
Principal Moments of Inertia with respect to Centre of Gravity:	I1:	0.004 kg m^2
	I2:	0.004 kg m^2
	I3:	0.007 kg m^2

Figure 21 – Input of physical attribute of Gripper Extension

To validate the model, the physical mass of the complete tool was measured at 1.956 kg using a digital scale. While a 176 g discrepancy exists, it appears that the modelled attributes are sufficiently accurate as when uploaded to the robot as seen above, the interruptions no longer occurred in subsequent trials.

8.2.   Calibration for Robot Operation

Further investigation uncovered that the mismatch in toolpath generation versus the active motion of the robot was primarily due to the inappropriate input of the "base" reference frame (base: X, Y, Z) and orientation highlighted in Appendix 4. This resulted in an incorrect spatial relationship between the robot's reference frame and that of the object of interest (i.e. the pin board mould). Hence it is essential that this input is accurate in order to correctly map the simulation with reality. Doing so establishes a means of correctly correlating general toolpath planning and execution within the workspace. Figure 22 illustrates the process used to achieve this mapping which involves manually calibrating this spatial relationship using the "3 Point" option in KUKA SmartPad.
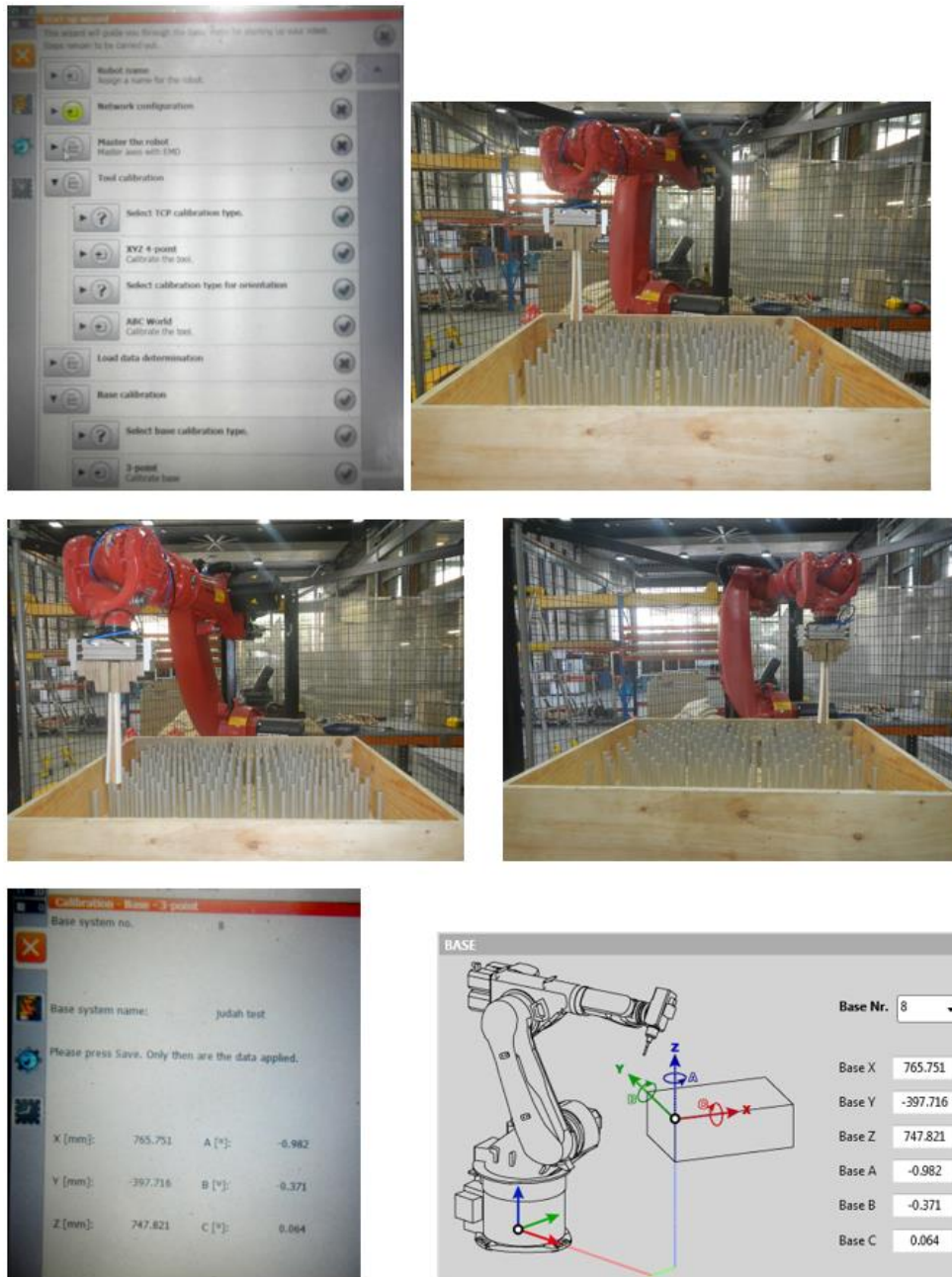
Figure 22 – Process for base calibration in order from left to right and descending.

Firstly, with the mould placed in the workspace, the tool tip is jogged to aligned with the origin pin ($n^{0,0}$) and the "calibrate" input selected to record this initial coordinate. The tool tip is then relocated along the desire X axis to the final pin of that row ($n^{12,0}$) and the position recorded before the final relocation in the XY plane to align with the final pin in the original column ($n^{0,23}$). At each step, the control cabinet records the rotational position of the six actuators. The kinematic equations that define the robots range of motion are internally solved using the data sets as variables. This calculation defines the location of the mould origin and it's orientation with respect to the robots own reference frame and produces the (base: X,Y,Z,A,B,C) values that are input into KUKA|PRC through the "Core Settings" functional block.

In conjunction with the previous improvement, further fine-tuning was required to ensure that the tool itself was reflected in the simulation and approached the target coordinates (pins) from the desired orientation (i.e. aligned with the longitudinal z-axis of the pins). Following a consult with the KUKA supplier, it was determined that the robot tool needs to manually calibrated.

Figure 23 – Process for tool calibration in order from left to right and descending

This is conducted using the "4 Point XYZ" option available through the KUKA SmartPad. Regarding Figure 23 the procedure involves incrementally jogging the robot actuators until the tool tip establishes minimal contact with a pointed landmark placed in the workspace. It is repeated four times with different orientations of approach and the discrepancy between the terminal flange and the landmark position is used to calculate the dimensions of the tool (tool: X,Y,Z) as well as it's orientation with respect to the terminal flange (tool: A,B,C). This is done automatically using the kinematic equations via the same process used to define the base

reference frame. Again this information is then required by KUKA|PRC for the simulation and is input by accessing the "Custom Tool" functional block.

9. Proof of Concept

This section serves to outline the efficacy of the concept, which was established by subjecting the first two panels of the ripple façade to all three stages from simulation to physically setting the mould and finally fabrication and assembly. Also discussed are the limitations associated with each stage, and the proposed solutions that, if implemented in future works would improve this prototypic fabrication concept.

9.1.   Optimisation and Evaluation of Algorithm

Through a process of trial and error along with additional research, a deeper understanding of the effective use Grasshopper and KUKA|PRC was obtained. Assessment of the algorithm used during the preliminary trail, identified redundant functional blocks and weaknesses. Several iterations of refinement resolved these issues to produce the final algorithm for the project included as Appendix 5. Significant changes include:

- Simplifying the generation of safety and surface planes for each pin by directly using the modified and original coordinate sets as inputs to the KUKA|PRC "Plane Orientation" functional block. The previous algorithm implemented unnecessary point deconstructions, a drilling depth slider and vector and perpendicular plane constructs to achieve the same result. This made the structure overly complicated and difficult to interpret.

- Accurate representation of the spatial relationships between the robot, tooltip and pin board mould achieved by uploading the calibrated base and tool reference frames previously discussed. Additionally by setting (tool: B) to -90^0 for both the robot and simulation the orientation of approach is constrained to align with the z-axis as desired. For astatic purposes, it was hoped that that the inventor model could be imported into Rhino however a cost effective solution does not exist at present. Due to time constraints, the tool extension was only partially remodelled. Functionally this has no impact on simulations, as the calibrated data is sufficient for the robot and software to interpret the tool. This is shown in Figure 24 as the white line protruding from the robot flange.

- Use of the KUKA|PRC "Weave" function which sequences the order of motions in each data stream by combining the linear translation of the first command with the respective translation of the next command and so on. By doing so the repetitive toolpath is redefined to undergo the same initial negative z-axis linear motion from safety to surface planes, however rather than a direct point-to-point motion to the next pin, the tool tip returns to the safety plane of the current pin. After which a third linear motion in the y-axis is responsible for subsequent alignment. This ensures that the tool tip does not collide with the pins during operation as illustrated by comparing Figure 19 and Figure 24.
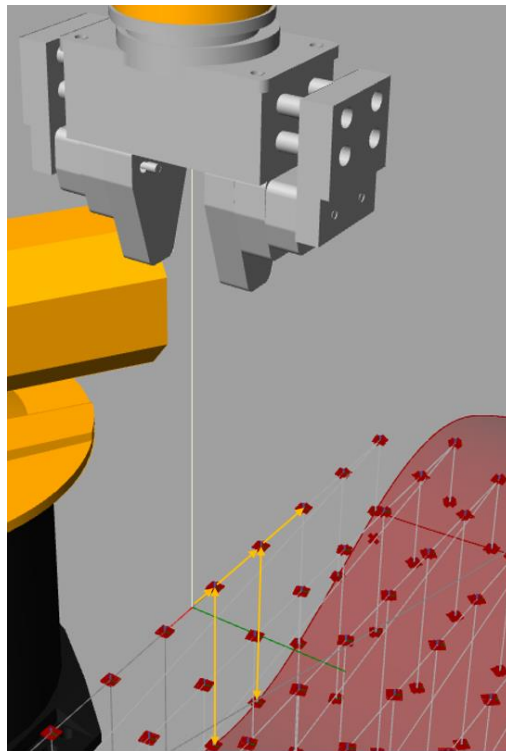
Figure 24 – Optimised simulation and toolpath

This Grasshopper file was used in the proof of concept for the first two panels and as seen in Figure 25 and Figure 26, the analysis of the simulations detected no collision or singularities for either. An excerpt of the KRL script for the first panel is included in figure to highlight the coding structure. Notice that setting of base-8 and tool-9 is automatically included and subsequently interpreted by the robot. Running the programs in the cleared workspace confirmed that the correct calibration of the machine had successful overcome the issues experienced in the preliminary trial.

```
14  ;FOLD STARTPOSITION - BASE IS 8, TOOL IS 9, SPEED IS 100%,
15  ;POSITION IS A1 5,A2 -90,A3 100,A4 5,A5 10,A6 -5,E1 0,E2 0,E3 0,E4 0
16  $BWDSTART = FALSE
17  PDAT_ACT = {VEL 100,ACC 100,APO_DIST 50}
18  FDAT_ACT = {TOOL_NO 8,BASE_NO 9,IPO_FRAME #BASE}
19  BAS (#PTP_PARAMS,45)
20  PTP  {A1 5,A2 -90,A3 100,A4 5,A5 10,A6 -5,E1 0,E2 0,E3 0,E4 0}
21  ;ENDFOLD
22
23  ;FOLD LIN SPEED IS 2.0 m/sec, INTERPOLATION SETTINGS IN FOLD
24  $VEL.CP=2.0
25  $ADVANCE=3
26  ;ENDFOLD
27
28  PTP {E6POS: X 0, Y 0, Z 100, A 0, B 90, C -18.181, E1 0, E2 0, E3 0, E4 0, S 'B 010'} C_PTP
29  LIN {E6POS: X 0, Y 0, Z 1.76, A 0, B 90, C -18.181, E1 0, E2 0, E3 0, E4 0} C_DIS
30  LIN {E6POS: X 0, Y 0, Z 1.76, A 0, B 90, C -18.181, E1 0, E2 0, E3 0, E4 0} C_DIS
31  PTP {E6POS: X 0, Y 50, Z 100, A 0, B 90, C -90, E1 0, E2 0, E3 0, E4 0, S 'B 010'} C_PTP
```

Figure 25 - Software Simulation for Facade Panel One with KRL script excerpt

Limitations

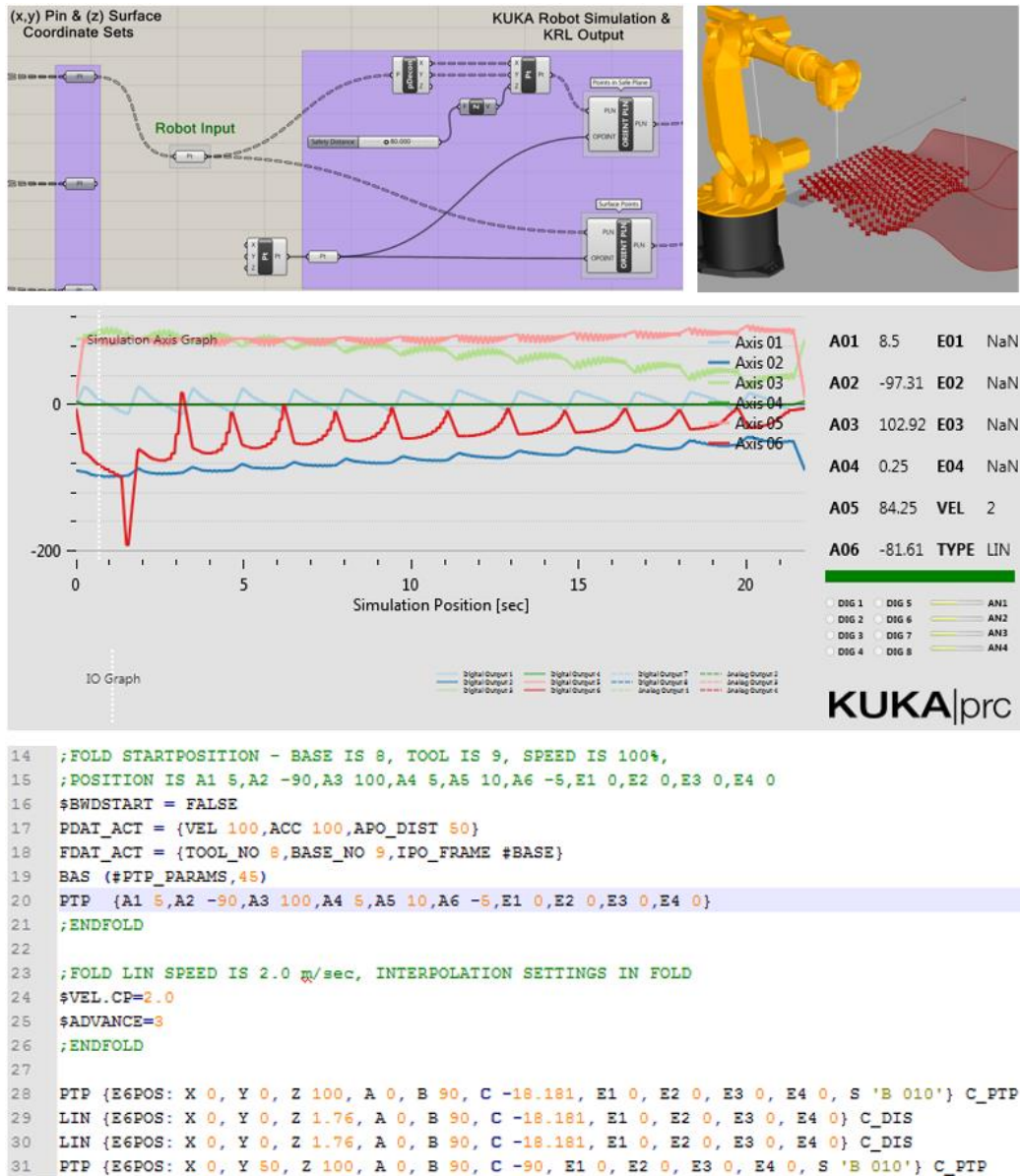A weakness identified within the algorithm is that when simulating the second panel, the reference origin is still associated with the surface geometry and not the robot. Hence, the coordinates for the second set of pins started with a 550mm offset in the y-axis. While not a problem in terms of the robots range of motion, it does cause a breach of the soft limits imposed and additionally required a base calibration specific for this panel. Attempts to overcome this by remodelling the algorithm to reproduce all panels at the location of the first (i.e. relative to robot reference frame) could not be completed due to time constraints. The most effective alternative solution involved manually offsetting the base used for the first panel by -550mm using the SmartPAD. Although effective, it is not a permanent solution

particularly for a mass, rapid production method, as it requires human intervention. Further development of the algorithmic approach must be considered in future works.
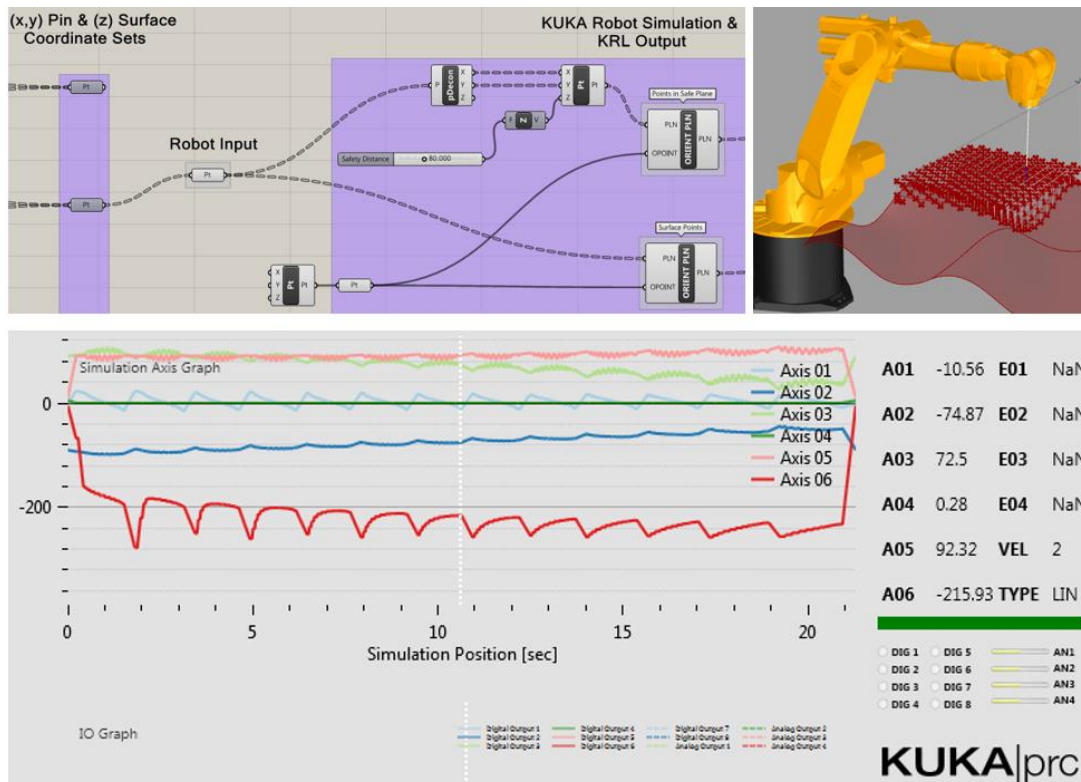

Figure 26 - Software Simulation for Facade Panel Two

9.2. Automated Mould Setting

The initial step in this process involves "zeroing" the mould to a datum plane by displacing the pins so that the non-plated end makes contact with the floor underneath. This is previously shown as the top right image of in Figure 12. This ensures that the displacement of the pins occurs from a common height and is essential for accurately setting the surface geometry. Once in place within the workspace, clamps fix the mould to elevated supports that provide adequate clearance from the table. While the interaction between the tool tip and the pins is smooth and seemly effortless for the robot, overcoming the friction in the mould during pin displacement can cause the structure to shift and some vibration does occur during operation, thus securing the mould is important. Additionally, if insufficient clearance is provided the pins are driven into the table with considerable force. During an initial test, this occurred and resulted in damage to the dowel of the gripper extension. Figure 27 shows the assembly of equipment during automated setting of the mould for the first panel.
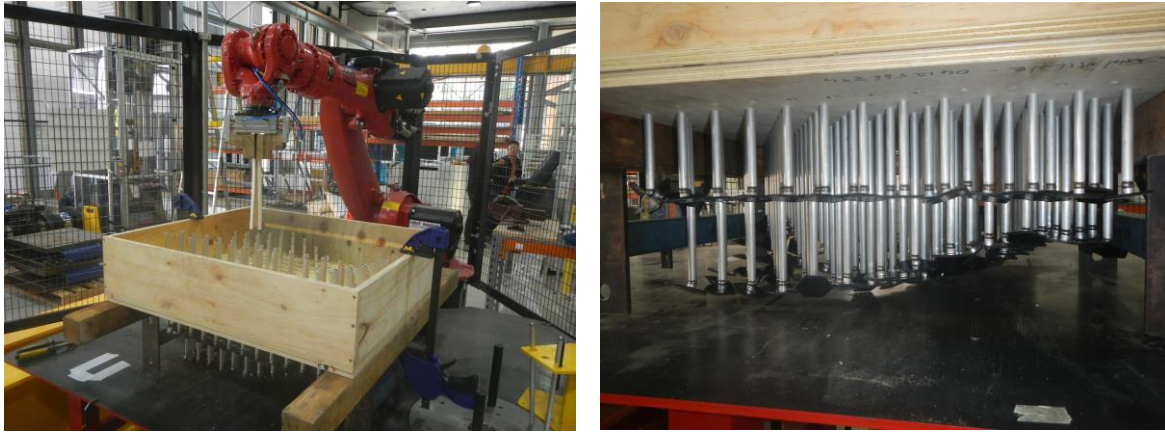
Figure 27 – Assembly of equipment (top) and progression of mould setting (bottom)

Results & Discussion

After running the program to completion, the resulting contour assumed by the mould bears a strong, visual resemblance to the under surface of CAD model as seen in Figure 28. This provides evidence that the Grasshopper algorithm can capture the surface geometry of the panel and transfer the coordinates defined by the dimensional parameters of the mould, to a KRL script during simulation to derive a robotic toolpath. It also proves that when run on the robot, base and tool calibration when applied with the gripper extension allow the machine to interact with the mould to replicate the simulation and establish the desired surface.
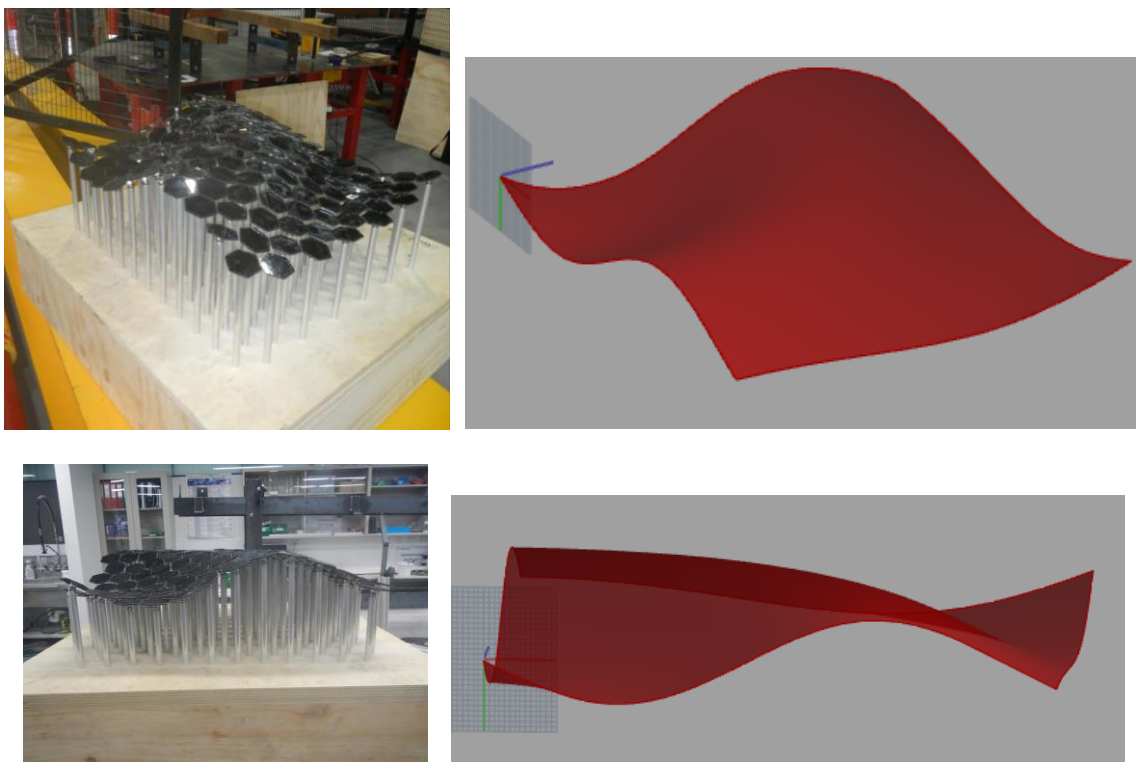

Figure 28 – Result of mould setting process (right) compared against similar perspective views of CAD surface geometry (left) for the first façade panel

An important factor for any manufacturing process is the tolerance to which a component can be produced. To determine the accuracy of the mould setting process, the height of the first pin, above the wooden frame was measured using Vernier callipers as illustrated in Figure 29. This provides a datum against which the relative displacement of 30 additional pins was found. These experimental measurements were compared against the analytically predicted z-axis coordinate of the relative pins obtained from the parametric equation. The assessment, included as Appendix 7 resulted in a mean error and standard deviation of 0.6 ± 0.83 mm.

Figure 29 – Method used to estimate tolerance associated with automated mould setting

Limitations and Potential Improvements

The following subsection outlines weaknesses related specifically to the automated mould setting process. Solutions are proposed for each limitation and provide opportunities for future development if the concept is to be cconverted into a full scale production method.

Tolerance

As previously seen in the specifications, the KR-16 has a pose repeatability of ± 0.05mm and its actuators have a rotational accuracy of 0.001°. Hence the error in pin placement is not due to the machine. In append… the largest difference between analytic and experimental height was observed for Pin ID 13 at 3.05mm and physically measuring the pin found it to be 5.0mm shorter to the majority. This was the case for multiple others where the disparities ranged from 0.5 to 5.0mm. Ensuring the pins are all a precise length would improve the tolerance of the mould setting process and thus the fabricated panels. Another potential source of error includes

that associated with the tool tip (±1.97mm) which could be reduced by a refining the gripper extension and a more stringent calibration.

Cycle time

The time taken to set the mould is approximelty 8 minutes. In the interest of safety, the six acutors are restricted to a rotational speed of 30 rad/s as previously dicussed. It is estimated that removing this limitation and allowing the robot to operate at the speeds shown in the specification, would result in at least a five fold reduction in cycle time. Whether this impacts the tolerance associated with pin placement is yet to be determined.

However, the most time consuming aspect of the concept specifically related to setting the mould stems from the transition from one panel to next. As the mould is removed from the workspace for its use in fabriation, the previously calibrated base is no longer suitable when assembling the equipment for the subsequent panel. Thus the mould needs to be re-zeroed, repositioned and the new base frame calibrated and refelcted in the simulation. This accounts for roughly 30 minutes of downtime between iterations. The following solutions propose a means of overcoming the cycle time of the process:

1. The need to reset the mould arises because the current system relies only on negavtive displacment of the pins. The design intent of the gripper extension was to physcially grip the pins themselves and provide enough static friction so that they could not only be pushed down by also pulled up along the z axis as seen in ....
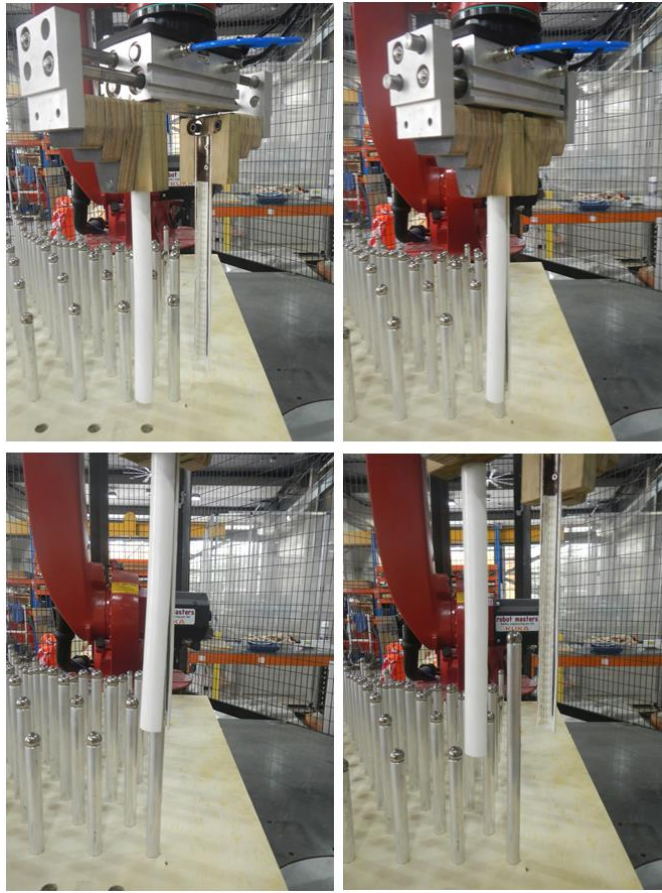
Figure 30 – Gripper extension capable of facilitating both positive and negative pin displacement.

Subsequently further modfication was made to the algorithm whereby an addional set of "Gripper close" planes is introduced between "Safety" and "Surface" planes. The extention to the Grasshopper code is provided in Appendix 6. At these points in the toolpath a 0.5 second pause repeates for all pins. Simultaneous, the compressed air gripper solenoid (Digital Output Four (DO-4)) received a "true" boolean command causing it to clamp shut and then continue with the negative dispalcement as before. When the motion is complete additional pause and "false" boolean commands are provided to cause the gripper to release the current pin and return to the respective safe plane as before. The underlying motivation is that rather that relying on the parametric equation alone to determine the z coordinates, the algorithm could be modified to calcuate the height difference between the pin locations for subsquent panels. Incoperating these differences would define a new starting point for each panel relative to the dispalcement associated with the previous panel and negate the need to zero the mould. While the modified algorithm performed as desired, the friction present between the board and individual pins is highly variable. Those considered stiff caused the occasional slippage of the pins

with respect to the clamped gripper extension which resulted in an inaccurate surface geometry. Increasing the rigidity of the 25mm protrution through the use of thicker steel rod and using a non-slip material with a higher coeffeicient of friction will resove this. Additionally, the mould could be refined by expanding the pin holes to allow a metal sleeve to be inserted with the pins. This will provide a more uniform static friction and also slow its progressive decrease due to cyclic wear.

2. The simplest way to overcome the need to re-calibrate and update the base between iterations would be to fix an adhesive grid to the table to provide references against which mould can be algined. However, a 12 mm inconsitency (diameter of dowel) in any direction causes the tool tip to miss the pins on descent. A more reliable solution should be acheived by perminently fixing a template frame in the workspace ensuring a constant spacial relationship with the robot. The mould can then simply be inserted into the frame.

9.3.   Façade Panel Fabrication

Having successfully set the surface geometry through automation, the next phase in establishing a proof of concept involved fabricating panel samples out of composite materials.

Preliminary Sample: Mould Limitations

As this was the first use of the mould, the purpose of this test was to assess its capability, identify fundamental issues and implement any rapid modifications necessary to provide core functionality. The modifications discussed below are considered temporary and provided a means of testing the prototypic concept to a level suitable for this thesis and stem from the following requirements:

- The mould needs to be airtight so that a standard vacuum can induce a negative pressure within the structure where the differential is significant enough to stretch a 5mm layer of silicon over the hexagonal plates to match the desired contour. Initially the gap between the pin board box and silicon frame was sufficient to equalise the differential thus the entire perimeter was sealed with putty.
- Once sealed several pins were negatively displaced because the frictional resistance of the mould and pin interface was less than the forces transferred through the plates as the silicon stretched in response to the vacuum. To overcome this a series of relief holes

were drilled into the frame which provides a means of controlling the pressure differential.

Figure 31 shows the assembly process for the first sample of panel one where the 5mm silicon sheet is drawn tightly over the hexagonal plates. The basic wet layup method was applied to form the laminate stack using a strip of hessian fabric topped by a layer of hemp based bio-composite and infused with approximately 1.5L of West System 105 Epoxy Resin and Group D Hardener in a 5:1 ratio. As the sample could only be checked infrequently, the precise curing time is unknown but is estimated to be 4 hours at most.

Figure 31 – Process for panel fabrication in order from left to right and descending.

While the resulting composite panel does resemble the CAD surface geometry, five major flaws are easily identifiable.

1. The low quality, patched appearance of the general surface finish occurred due to inadequte infusion of the epoxy resin. Vacuum bagging the samples over hand laying would solve this issue however time constraints prevented the application of this method. The inconsistent surface finish is less prevalant for the strip of hessian thus revising the materials used was determined as the most practical alternative to vacuum bagging.

2. The hexagonal pattern is clearly visable on the fabricated panel. While the ability to imprint patterns on a façade may be of interest to some for asthetic purposes, in the context of this project a smooth finish was desired. To achieve this, six layers of cotton cloth were placed over the hexagonal plates during the fabrication of additonal samples.
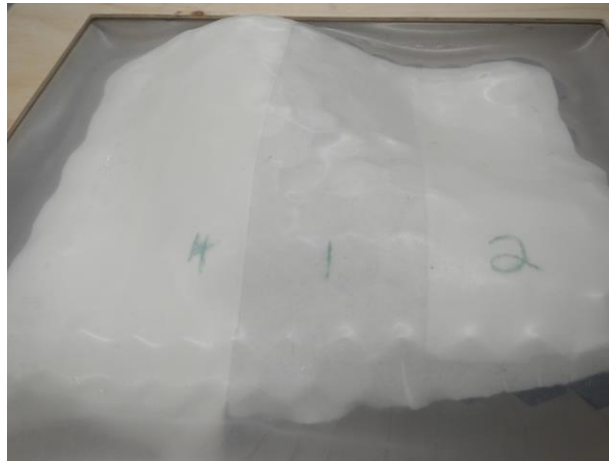

Figure 32 – Improving surface smoothness using increased layers of cloth.

3. Analysing the hexagonal pattern found that several imprints were either raised or depressed in comparison to those surrounding. This indicated that prolonged exposure to the forces induced by the vaccum caused the gradual displacement of certain pins. For those easily manipulated by hand, a screw was inserted through the frame at an angle to induce a shear force to fix the respective pin in place once set. Additionally, 1mm clear plastic, which conforms to the surface at lower pressures, was used in place of the silicon.

4. Due to the gradient of curvature of the ripple, hexagonal plates distributed along the local minima of the surface were forced to overlap while those found at the maxima had a greater spread. Those that overlapped resulted in an uneven surface however inclusion of the six layers of cloth minimises the discrepancy
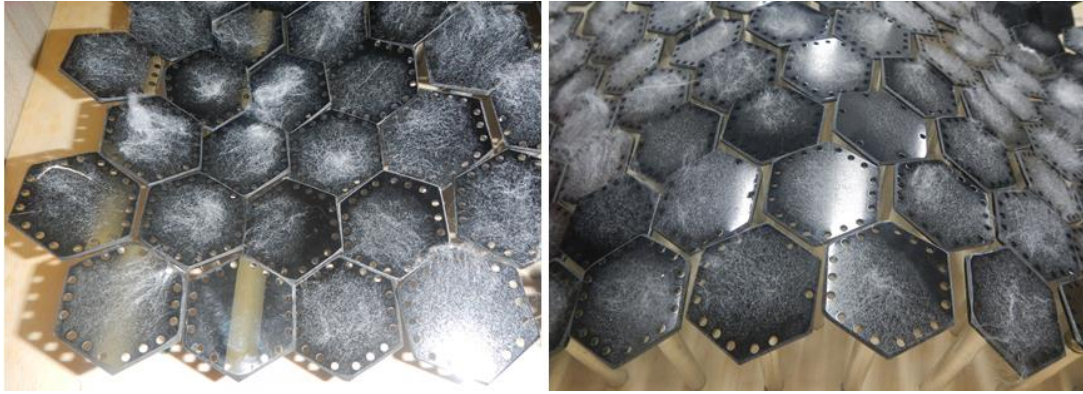
Figure 33 - Comparison of plate spacing at local minima (left) and maxima (right)

5. The final limitation of the mould uncovered through the preliminary test, is that the flexible layer used to contour the surface causes the boundary pins to deflect inappropriately. They assume an orientation that matches the curvature developed between the frame that secures the silicon which is dependent on how high the support frame is set above the pin board box. This causes the resulting perimeter of the panel to be distorted from the desired geometry. Again, the severity of this is reduced by applying the cloth and using plastic over silicon which has less potential to displace the plates.

1.1.3   Results & Discussion

In terms of material selection, the revised laminate consists of a single layer of 550gsm, Biotex Jute 2x2 twill weave topped by two orthogonal layers of hessian. The first panel is set in polyester resin with 6% wax in styrene to provide a glossed surface finish and is estimated to have taken two hours to cure. The second made use of the epoxy resin previously dicussed and due to the different materials used took approximatly three hours to cure as opposed to four . An additional rational behind changing the materials is that the samples show a variety of composites can be used in this concept for fabrication.

Figure 34 – Improved sample for first panel.

By overcoming the obstacles associated with the preliminary test, improved samples were fabricated. Following curing of the second sample panel, post processing invloved cutting both panels to size to remove excess material. The 25mm excess on the matching edges for each panel, present due the offset of the hexagonal plate grid which serves to ensure that the curvature between panels is continuous was trimmed from panel two but kept for panel one. This provided a portion of reference material used to align and secure the panels together by overlapping the panels 25mm. Once assembled, a strong visual correlation as seen in Figure 35 is present where general curvature of the façade section clearly resembles that of the CAD modelled surface.

Figure 35 – Assembly of two sample panels.

Limitations and Potential Improvements

A close individual and comparative inspection of the fabricated panels reveilved a series of defects that the temporary improvements had failed to fully address. While the surface finish is improved through the use of the cloth underlay, inconsitencies are still present and imprints of the deformation associated with streching the plastic are visible. This reinforces the need for vacuum bagging samples in future. Localised non-uniform regions of curvature are still present due to pin dipalcement although less pronouned than before. This is also be due to fact that some pins were physically shorter than others contributing to the 0.6mm error dicussed in automated mould setting.

Again, the most concerning functional limitation of the mould is that the perimeter plates are deflected based on the contour of the plastic causing an inconsistent geometry with repect to the boundary of the CAD model. This causes a partial mismatch between the married edges of the two panels shown below.

Figure 36 – Defect between panels.

While curing of the second panel was underway, the pressure diferential within the structure caused the plastic to creep and eventually rupture. Equilibration of pressure allowed the layers of cloth to expand which reduced the gradients of curvature for this samples. Ultimately this contributed to less pronounced maxima and minima and also the inconsisent transition between the edges of panels one and two seen previously.

Mould Design Optimisation

Based on the observations made during fabrication and assembly of the second batch of samples, two major design modifications were conceived to improve the capability of the mould.

An effective locking mechanism is required to ensure that all pins remain in place once set even under prolonged exposure to the vacuum. The design for a potential system is illustrated in Figure 37 and relies upon an additionally layer of timber mounted to a rail system on the underside of the pin box frame. This 600 x 700mm timber panel will have key holes that align with the pins and formed by 7.5mm offset 15mm and 12mm diameter holes. Once the pins are set, by rotating the locking screws, the panel will be linearly displaced until the 12mm section of the keys induces a shear force against the lower pin shafts to fix the mould. This will allow a greater negative pressure to be induce in the structure to potentially stretch a thicker layer of silicon over the pins to provide an optimal moulding surface and negate the need for the cloth to remove the hexagonal imprint.
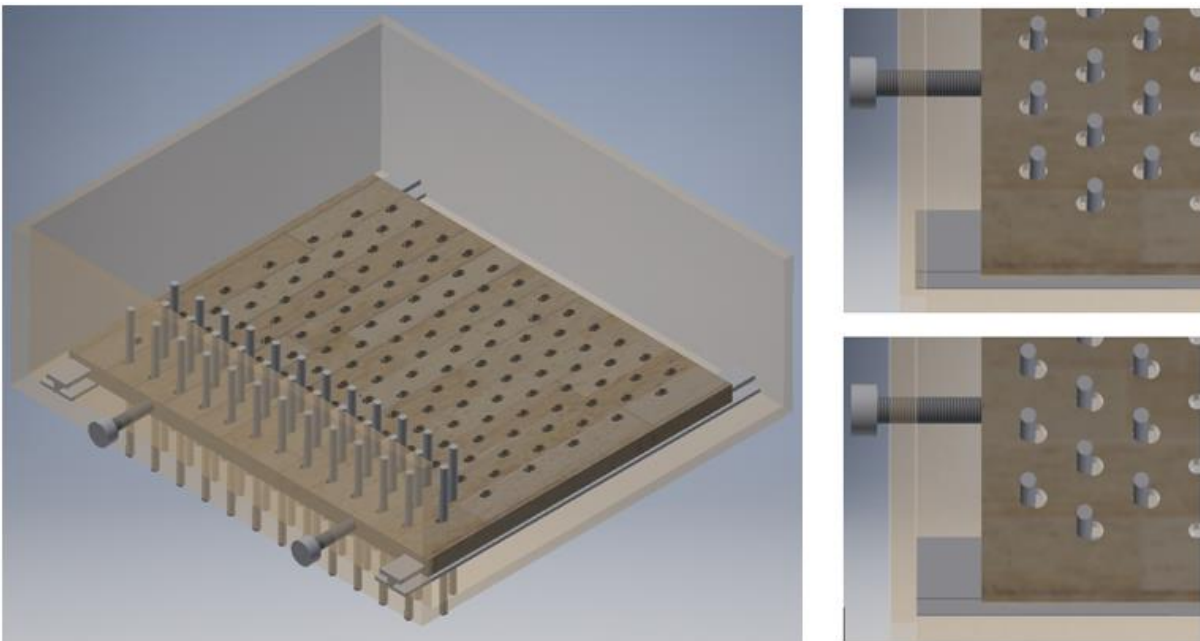

Figure 37 – Proposed locking mechanism

To ensure that the orientation of boundary plates remains consitent with the desired geometry additional pins need to added to the current perimeter. These pins will be non plated and placed so that their top surface can establish contact with the adjacent hexagon. Once the mould is set and locked, the perimeter pins will provide support from below the plate to oppose the force generated by the silicon layer and prevent rotation about the ball bearing for the boundary plates. It is expected that the continuation of the surface curvature between neighbouring panels

of the façade, will be significantly improved through the use of this mechanism. Figure 38 provides an illustration of the design modification for a single corner pin.
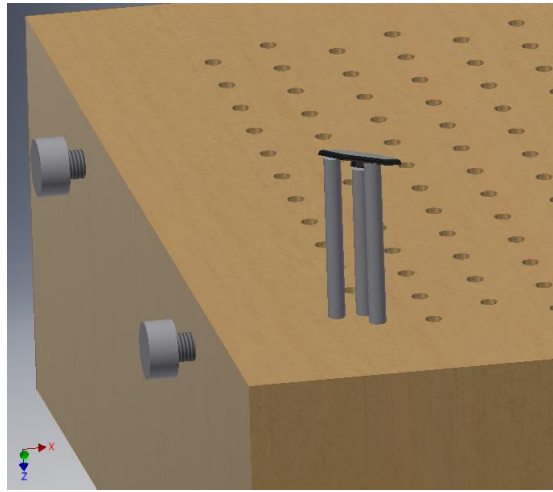

Figure 38 – Support pins around perimeter to prevent boundary plate deflection

Additional minor design changes that should be considered are:

- Including a window in the side of the pin box frame topped by a sliding gate mechanism to provide controlled relief of the vacuum pressure.

- A four-latch locking mechanism to secure the base of pin box frame to the rest of the structure. At present the base is screwed in place and as the robot displaces the pins from the under surface, the base needs to be removed and replaced for each panel which adds to cycle time.

- Increasing the depth of the silicon layer support frame by 75mm will provide sufficient clearance between the pins and the table during automated mould setting. This would allow the two components to be permanently fixed and sealed into a single unit without compromising functionality. This would remove several tedious, time consuming steps such as the need to clamp the mould in robot workspace as well as various assembly related tasks.

10. Conclusions

In addressing the aim of this thesis, several applications relative to 3D CAD modelling, coding and robotic simulations were assessed against a variety of criteria. The selection was primarily based upon: cost, presence of native KUKA robot models and capability to import CAD files; availability of education resources and support; the ability to simulate toolpaths and derive KRL scripts from them.

 Rhinoceros 5, the visual programming plug in, Grasshopper and the robotic simulation extension, KUKA|PRC proved to be the most suitable combination of digital tools for this project. The Grasshopper algorithm, created by Ting Lee and Joe Gattas, used to model and panalize the ripple façade from the defining equation and dimensional parameters of the mould, provided a solid foundation for the project. A combined effort in assessing KUKA|PRC resulted in an algorithm that could conduct robotic toolpath simulations and generate machine driving KRL script which marked the completion of the first objective.

While preliminary trials proved unsuccessful, each failure provided insight into operational requirements of the robots, opportunities for improving the algorithm and the need for a suitable tool extension which was subsequently design and fabricated. By determining the processes behind calibrating the robot, an accurate spatial relationship was established with the mould and tool respectively. Once uploaded to KUKA|PRC, a match between simulation and reality was achieved.

The potential of the algorithm arises because the dimensional parameters of the mould implicitly constrained its coding. Thus, the same Grasshopper file can now be used by UQ staff and students to rapidly evaluate a variety of parametrically designed surfaces where the only change required is the input of the equation or its underlying independent variables. This is automatically reflected in the simulation component of the coding and so generating KRL script to prototype different façade panel designs is effortless. To illustrate this potential, parameters of the defining ripple equation (Equation 1) are altered to the values of Equation 2 alongside the resulting geometry and toolpath

$$140 \times 0.6 \sin \left\{ \sqrt{\left(\frac{x + 300}{1.6 \times 10^{-2}}\right)^2 + \left(\frac{y - 1.5}{1.6 \times 10^{-2}}\right)^2} \right\}$$
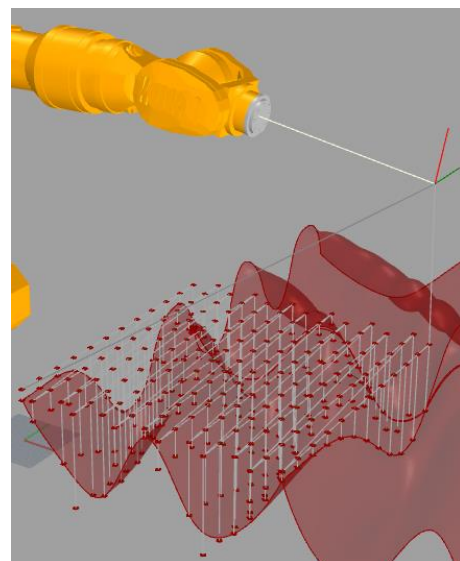
Equation 2 – Modified Parametric Equation   *Figure 39 – Updated Surface and toolpath*

The resulting KRL scripts can successfully instruct the robot along an optimised toolpath and displaced the pins of the mould to within 0.6mm of the desired coordinate on average. This primary source of error is not associated with the machine or algorithm but stems from inaccuracies of the mould (up to 5mm discrepancy in pin length) and gripper extension prototypes (±1.93mm). Setting the mould is expected to take less than 2 minutes at fully operational speed. This may negatively impact the accuracy or result in unforeseen consequences such as damage to the mould and so should be addressed carefully in future works. The outcome of accurately setting the mould for the first two panels of the ripple facade marks the first instance where a KUKA robot in UQ's possession has successfully fulfilled its function within a project and satisfies the requirement of the second objective.

The composite façade panel samples produced by the mould and thus this concept are admittedly of a lower quality than would be achieved through conventional formative, additive or subtractive techniques. While the general curvature of the panels correlated well with both the CAD geometry and each other, numerous surface defects are present and there is a noticeable mismatch between the married edge of the two panels. However, a positive result is obtained through a comparison between the preliminary and final samples. A significantly improved surface finish was obtained using basic modifications to the mould and altered materials.

At present the concept could not be considered as a rapid, mass manufacturing method. This partially is due to the poor product quality previously discussed but also because of long cycle times. The second sample for the first panels was fabricated in the least time. From calibration of the base to removal of the cured mould it's estimated to have taken 3.5 to 4 hours. Based on this only two to three panels could be produced per day. The most significant contributions stem from reassembling the mould, hand laying the composites and the time required to cure.

Regardless, the assembly of the two-neighbouring composite façade panel samples, provides evidence that this concept is a viable, cost effective and environmentally friendly means of producing digitally designed facades with highly variable, double curved geometries through the integration of robotic automation and a reusable, adjustable mould.

10.1. Future Directions

This report identifies limitations at each stage of the process which are address by suggested improvements such as extending the algorithm to include bidirectional pin placement, a variety of mould design improvements and the need to vacuum bag samples. It is hoped that

these improvements which aim to reduce cycle times and improve product quality, will be taken on-board during future research and development of this concept so that its full potential can be realised. Unfortunately, delayed access to the robots along with a steep learning curve and a lack of timely support from KUKA Robotics as well as unexpected complication with the moulding process lead to time constraints that prevented secondary goals from being achieved.

It was hoped that all eight panels of the ripple façade could be fabricated and assembled during which additional flaws would have been exposed. The continuation of this project along with implementing the recommendations of this report will serve to bolster UQ's knowledge base on KUKA robot operation.

A major limitation of the results presented in this thesis is that the comparison between the fabricated panels and CAD model relies on a qualitative visual assessment. It was the intent to use the Faro 3D scanning technology to obtain point clouds for each panel and compare the percentage of overlap between the scanned and original to assign a quantitative value of tolerance for the holistic concept. This provides an opportunity to determine the current status quo of product quality as well as the efficacy of the improvements made by assessing scans of the panels discussed in this paper against the model along with the point clouds obtained for subsequent panels.

11.   References

AutoDesk, Inc. (2016). *Various pages of parent website*. Retrieved from DynamoBIM.org: http://dynamobim.org/

Boers, S. (2016, April 5). *Optimal Forming*. Retrieved from http://www.optimalforming.com

Caneparo, L. (2014). *Digitital Fabrication in Architecture, Engineering & Construction.* Springer.

Davidson, S. (2016). *Various pages of the parent website*. Retrieved from Grasshopper - Algorithmic Modeling For Rhino: http://www.grasshopper3d.com/

Ginkel, L. V. (2010). *Rapid Manufacturing in facade design : Case study to an innovative shading device.*

Issa, A. P. (2009). *The Grasshopper Primer, Second Edition.* Robert McNeel & Associates.

Knaack, U. (2007). *Facades: Principles of Construction.* Berlin: Die Deutsche Bibliothek.

KUKA Robotics Pvt Ltd. (2016). *Various pages of the parent website*. Retrieved from KUKA Robotics Australia: http://www.kuka-robotics.com/en/company/

Llinares-Millan, C. (2014). *Construction and Building Research.* Switzerland: Springer.

McGee, W. (2014). *Robotic Fabrication in Architecture, Art and Design.* Springer.

Nguyen, Q. (2013). *Composite Materials for Next Generation Building Facade Systems.* Melbourne: Horizon Research Publishing.

Park, H. K. (2015). Developing the Preliminary Estimate for the Free-Form Building Facade in Conjusction with the Panel Optimization Process. *KSCE Journal of Civil Engineering*.

Pronk, I. A. (2009). Double-curved surfaces using membrane mould. *Proceedings of the International Association for Shell and Spatial Structures (IASS) Symposium.* Valencia.

Pronk, I. A. (2015). Flexible mould by the use of spring steel mesh. *Proceedings of the International Association for Shell and Spatial Structures (IASS).* Amsterdam.

Robert McNeel & Associates. (2016). *Various pages of the parent website*. Retrieved from Rhinoceros 3D: https://www.rhino3d.com/

Spring, M. (2007, Issue 47). *Innsbruck cable car stations: Zaha Hadid lifts the spirits.* Retrieved from Building.co.uk: http://www.building.co.uk/innsbruck-cable-car-stations-zaha-hadid-lifts-the-spirits/3100491.article

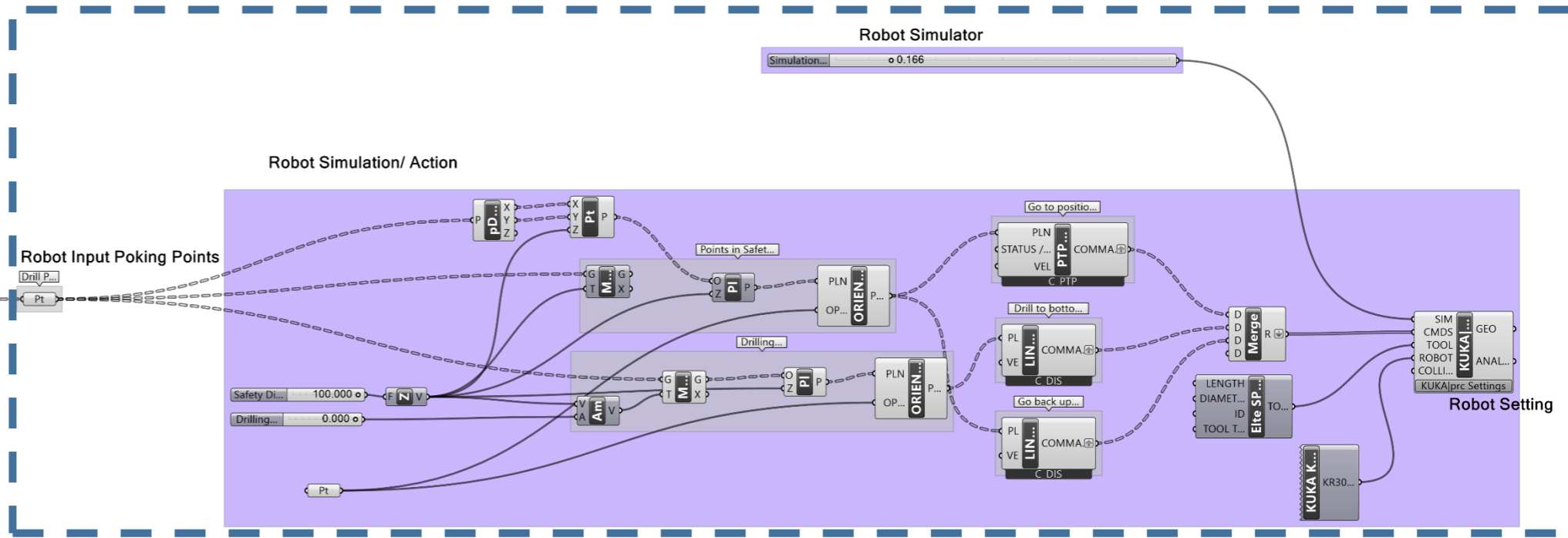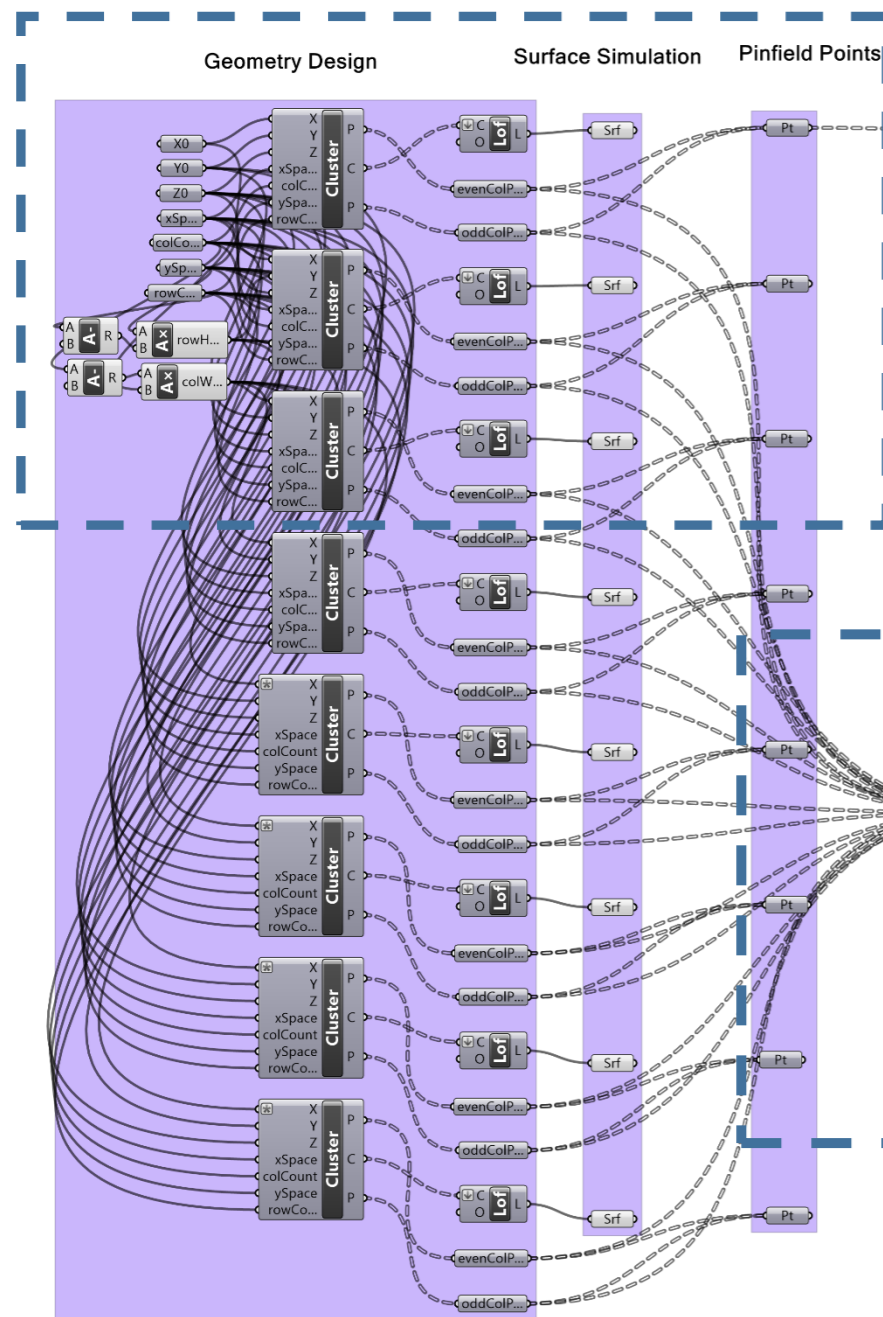Tasmanian Government, Department of Premier and Cabinet . (2011, December 6). *Project Management.* Retrieved from Tasmanian Government: http://www.egovernment.tas.gov.au/project_management
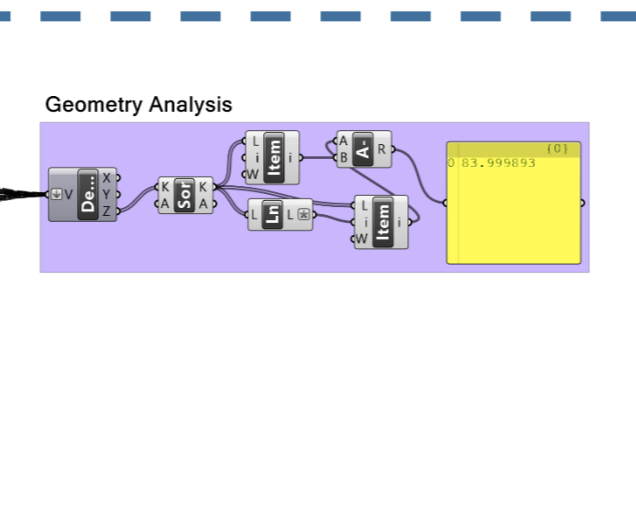
UQ - School of Civil Engineering. (2016). *The Civilian Handbook v1.1.* Brisbane.

Appendix 1 - Hollistic Grasshopper Algorithm: Preliminary Version.

See Appendix 4

Geometry Design

Surface Simulation

Pinfield Points

Robot Simulator

Robot Simulation/ Action

Robot Input Poking Points

Points in Safet...

Go to positio...

Drilling...

Drill to botto...

Safety Di...   100.000

Drilling...   0.000

Go back up...

Robot Setting

See Appendix 6

Geometry Analysis

0 83.999893

Functionality is redundant.

Appendix 2 - Detail of ripple façade modelling and pin board correlation.

Establishment of zero coordinate and façade model grid on which each panel is mapped from the Geometry Cluster.

"Lofting" parametrically modelled NURBS curves into surfaces to form each panel. Provides visual representation of surface in Rhino

Extracting Pin Board coordinate sets per panel for use as robot input coordinates.
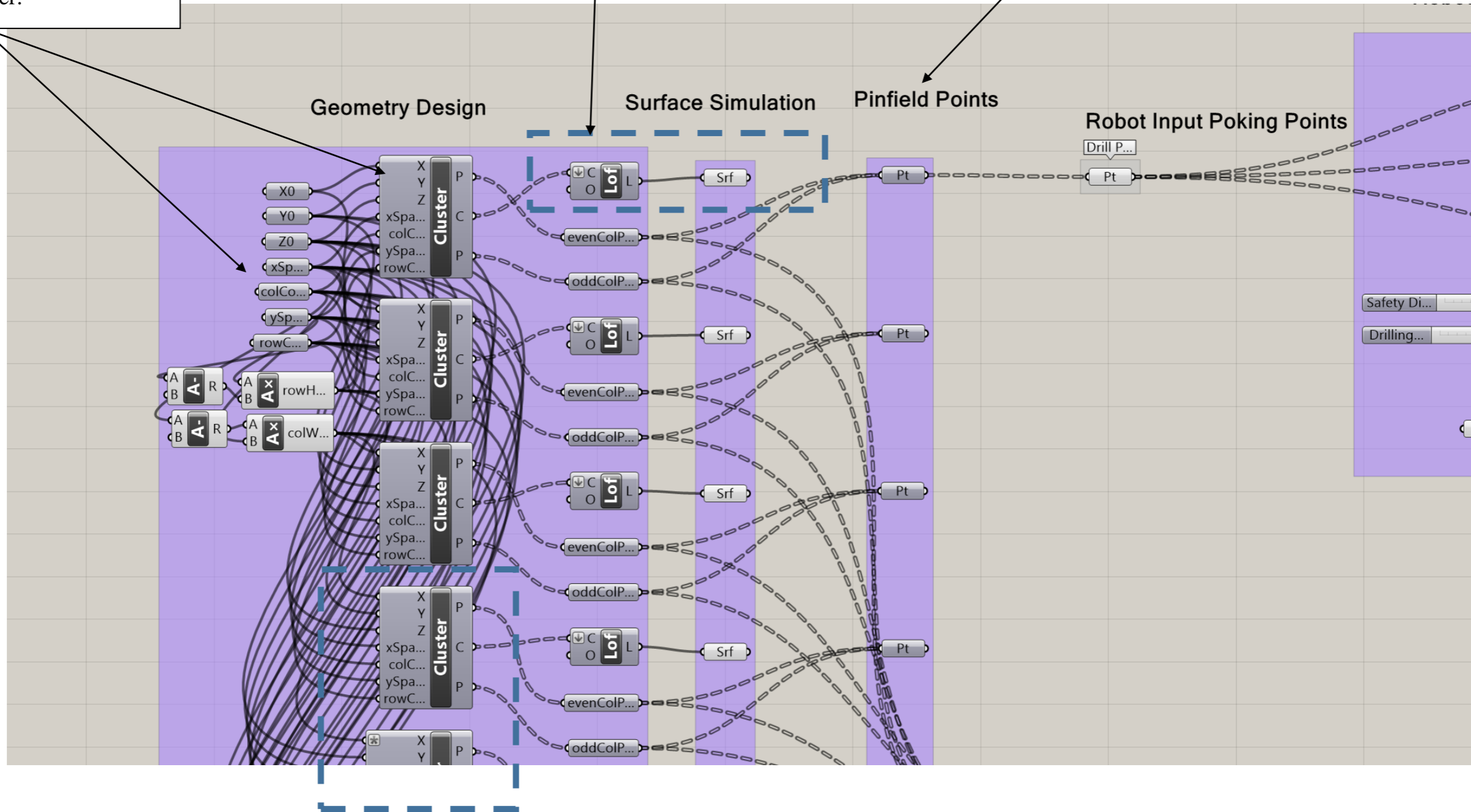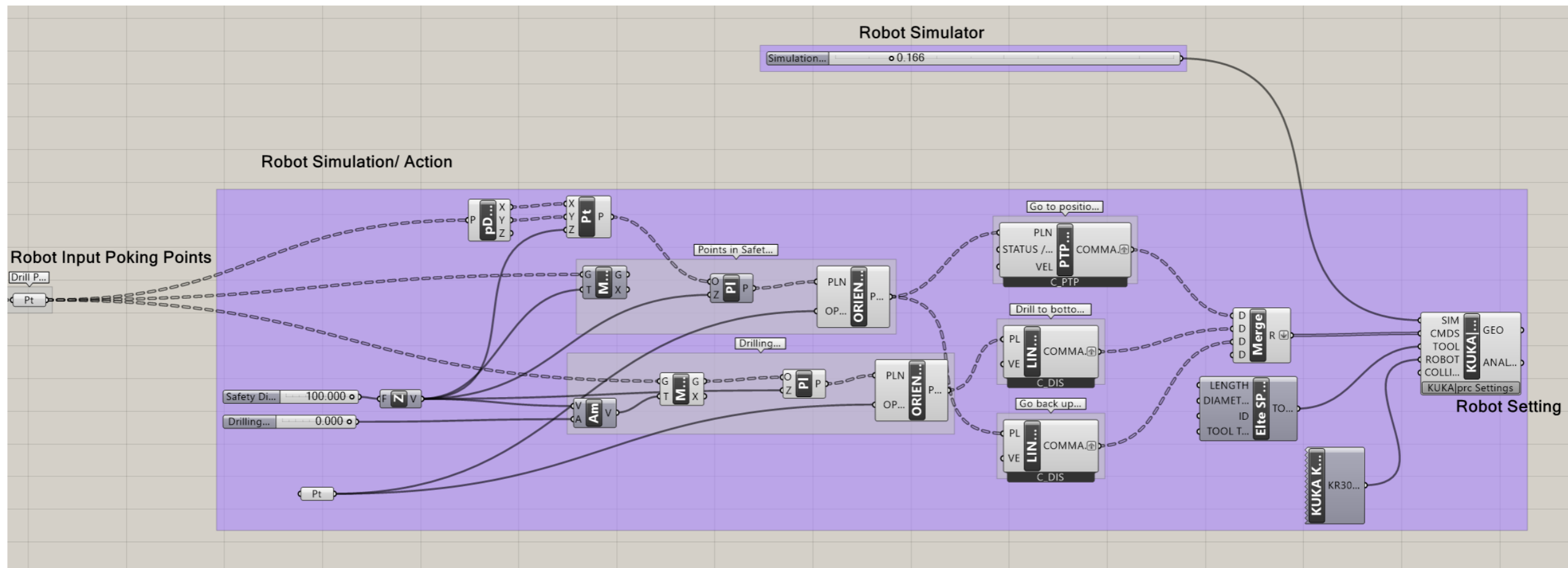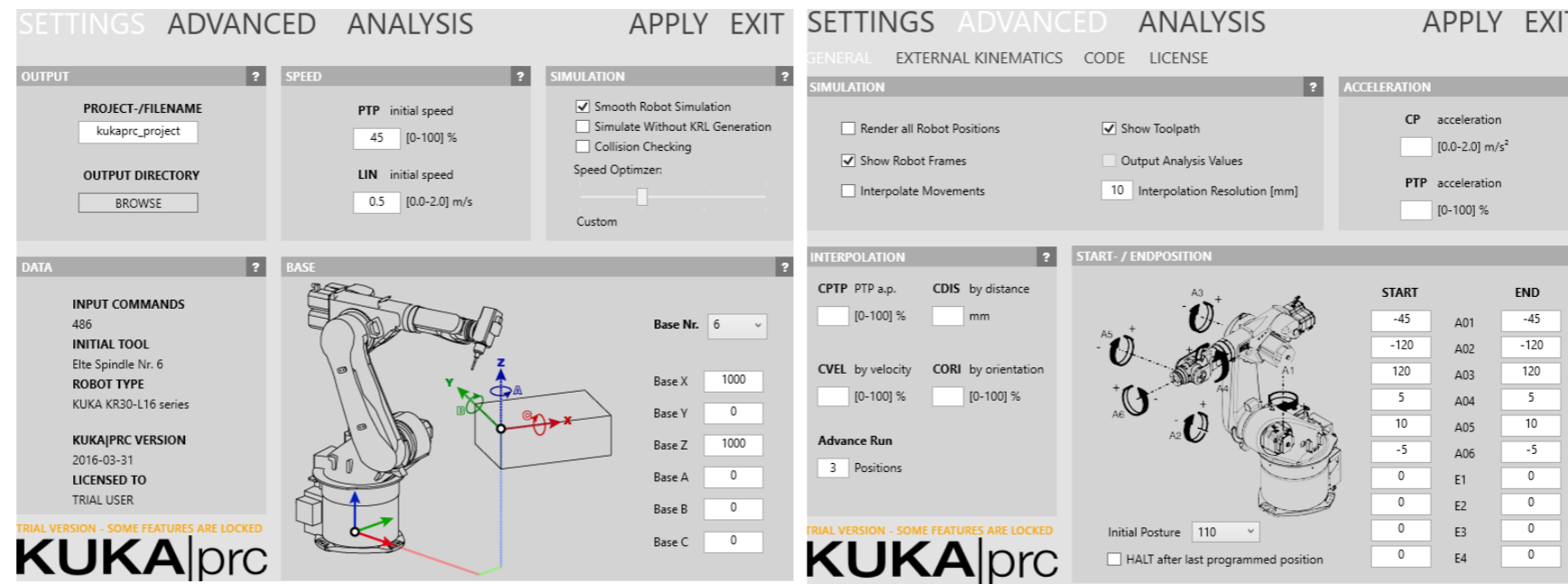
See Appendix 5

Evaluation of the parameter equation using x,y coordinates previously generated in order to derive the corresponding z coordinate of the surface for each point.
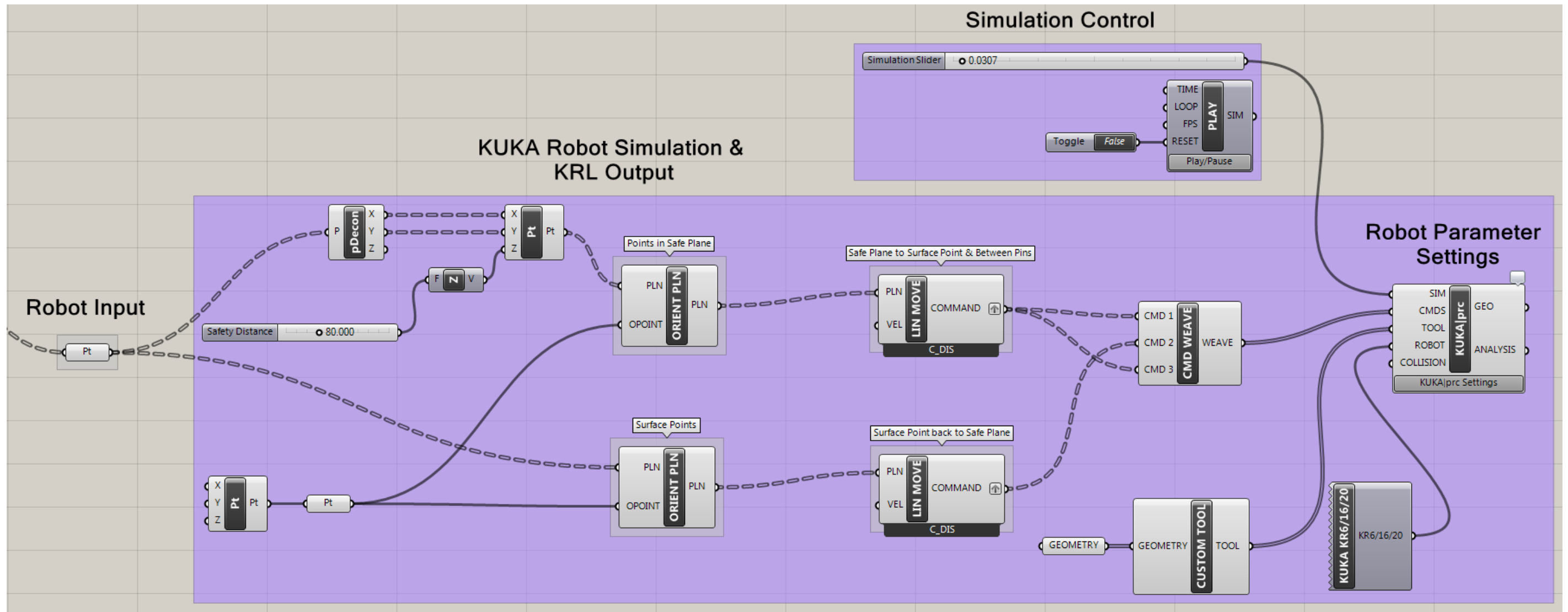
Output of the points and interpolation to form a curve for use the in the parent code in Appendix 3.
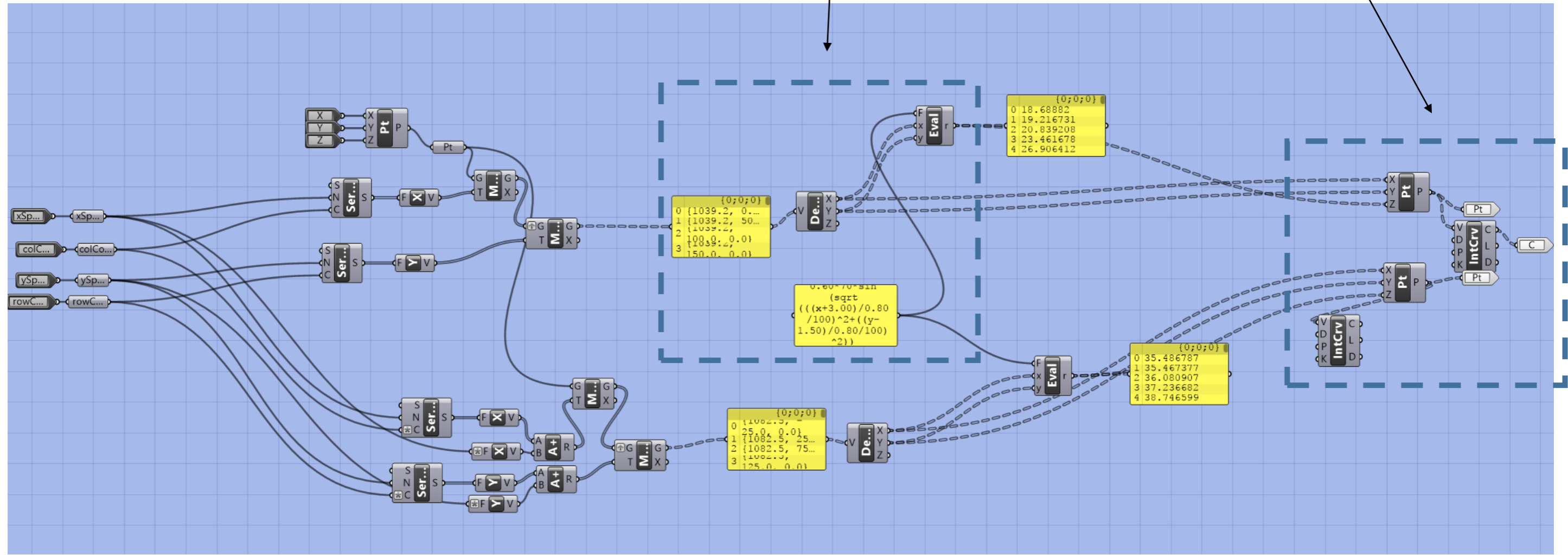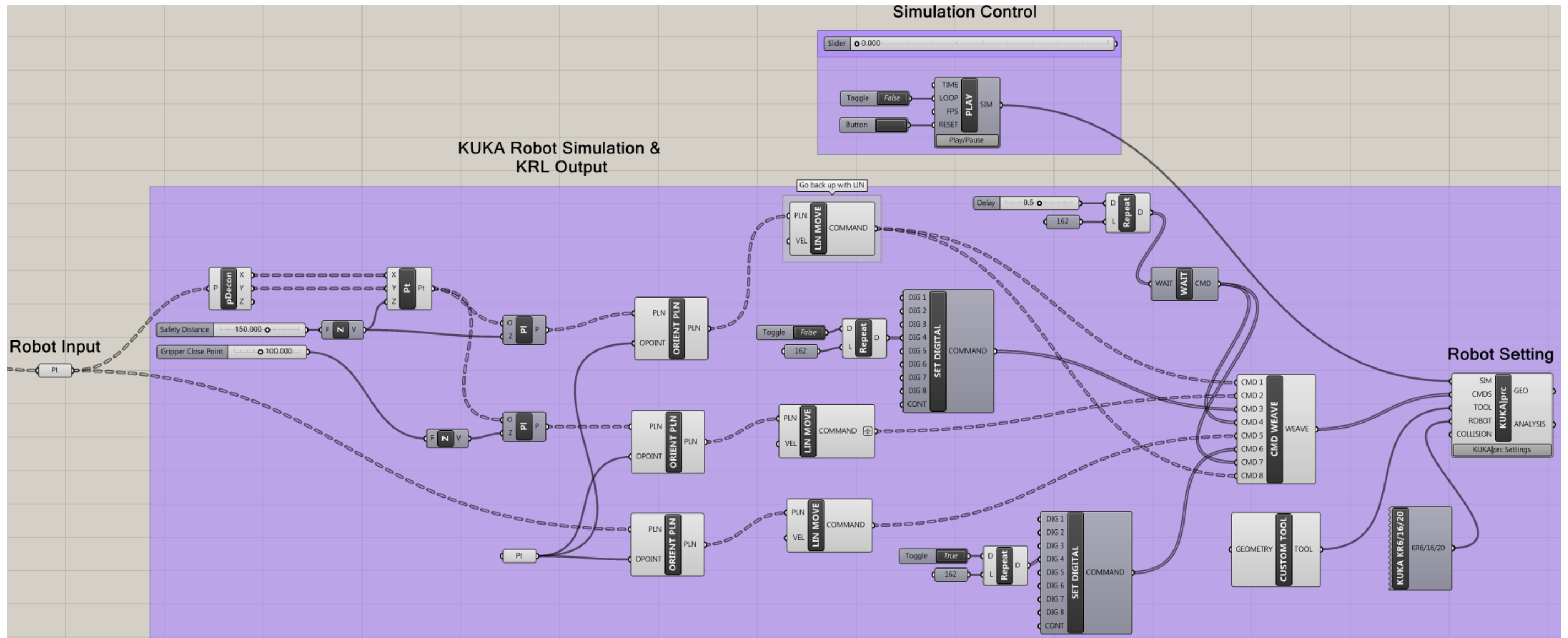
Appendix 4 - KUKA.PRC derived algorithm for preliminary robotic simulation.

Appendix 5 - Grasshopper Simulation Algorithm: Final Version.

Appendix 7 – Mould Setting Tolerance Assessment

PIN ID	Analytic z-axis Value	Measured z-axis Value	Height Difference w.r.t. Ref Pin (ID:1)	Absolute Analytic vs Actual Height
1	1.760	99.22	-	-
2	23.971	75.66	23.56	0.41
3	39.610	59.84	39.38	0.23
4	40.296	58.87	40.35	0.05
5	25.753	73.33	25.89	0.14
6	1.475	97.90	1.32	0.15
7	-23.362	119.10	-19.88	3.48
8	-39.367	139.06	-39.84	0.47
9	-40.490	139.29	-40.07	0.42
10	-26.305	125.87	-26.65	0.35
11	-2.176	101.25	-2.03	0.15
12	22.776	76.18	23.04	0.26
13	37.807	58.36	40.86	3.05
14	40.158	59.58	39.64	0.52
15	41.816	57.28	41.94	0.12
16	34.731	65.07	34.15	0.58
17	17.098	81.64	17.58	0.48
18	-6.708	106.48	-7.26	0.55
19	-28.755	128.32	-29.10	0.34
20	-41.038	141.45	-42.23	1.19
21	-38.795	138.38	-39.16	0.37
22	-22.528	121.83	-22.61	0.08
23	2.012	96.88	2.34	0.33
24	25.881	73.35	25.87	0.01
25	33.893	65.82	33.40	0.49
26	31.752	68.29	30.93	0.82
27	24.345	74.30	24.92	0.57
28	10.846	88.09	11.13	0.28
29	-7.361	106.57	-7.35	0.01
30	-25.958	124.10	-24.88	1.08
31	-39.010	140.08	-40.86	1.85
			Average Error	**0.63**
			STD DEV	**0.80**

KR 30 L16-2

Work envelope[1]	Dimensions A	Dimensions B	Dimensions C	Dimensions D	Dimensions E	Dimensions F	Dimensions G	Volume
KR 30 L16-2	3,567 mm	4,992 mm	3,102 mm	2,017 mm	1,085 mm	2,050 mm	1,545 mm	104.5 m³
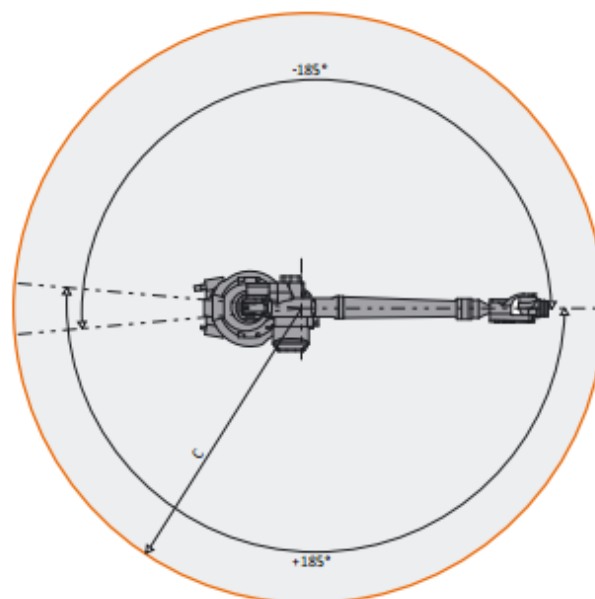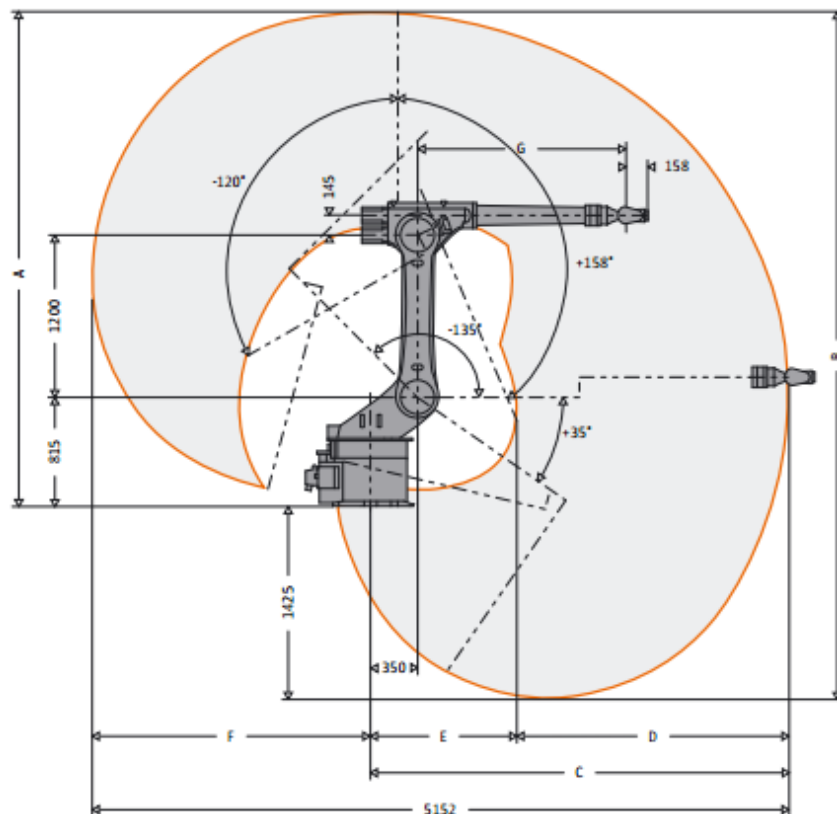
[1] Relative to intersection of axes 4/5.

KR 16-2

Work envelope [a]	Dimensions A	Dimensions B	Dimensions C	Dimensions D	Dimensions E	Dimensions F	Dimensions G	Volume
KR 16-2	2,026 mm	2,412 mm	1,611 mm	1,081 mm	530 mm	1,027 mm	670 mm	14.5 m³
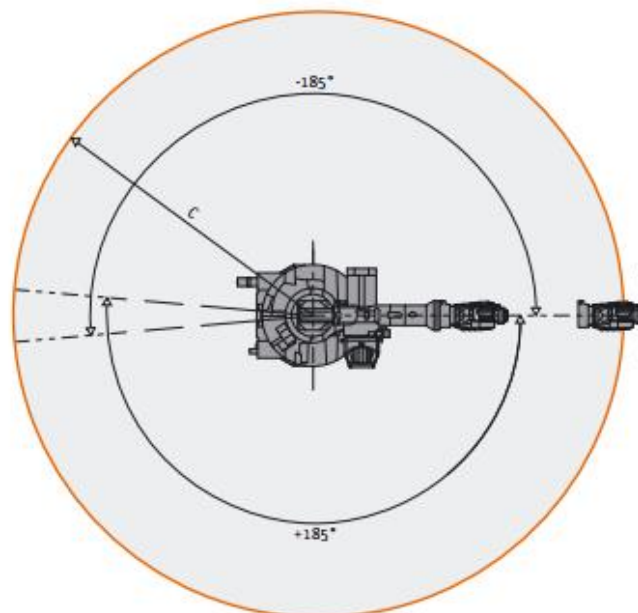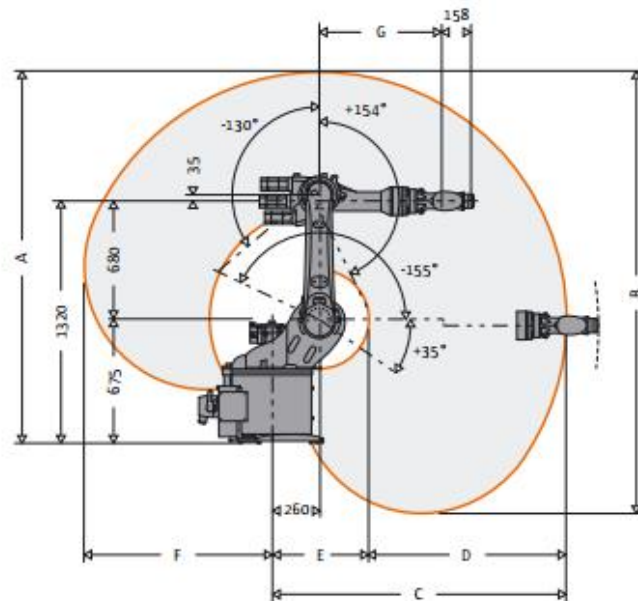
The work envelopes are credited to the respective KUKA robotics specification documents.